Contaminant Hydrogeology

C. W. Fetter

Department of Geology
University of Wisconsin–Oshkosh

Macmillan Publishing Company
New York

Maxwell Macmillan Canada
Toronto

Maxwell Macmillan International
New York Oxford Singapore Sydney

reactions. These can be either (1) surface reactions, such as hydrophobic adsorption of neutral organic compounds and ion exchange of charged ions, or (2) classical chemical reactions such as precipitation and dissolution.

3.3 Sorption Processes

Sorption processes include adsorption, chemisorption, absorption, and ion exchange. **Adsorption** includes the processes by which a solute clings to a solid surface. Cations may be attracted to the region close to a negatively charged clay-mineral surface and held there by electrostatic forces; this process is called **cation exchange.** Anion exchange can occur at positively charged sites on iron and aluminum oxides and the broken edges of clay minerals. **Chemisorption** occurs when the solute is incorporated on a sediment, soil, or rock surface by a chemical reaction. **Absorption** occurs when the aquifer particles are porous so that the solute can diffuse into the particle and be sorbed onto interior surfaces (Wood, Kramer, and Hern 1990).

In this chapter we will not attempt to separate these phenomena but will simply use the term sorption to indicate the overall result of the various processes. From a practical view the important aspect is the removal of the solute from solution, irrespective of the process. The process by which a contaminant, which was originally in solution, becomes distributed betweeen the solution and the solid phase is called **partitioning.**

Sorption is determined experimentally by measuring how much of a solute can be sorbed by a particular sediment, soil, or rock type. Aliquots of the solute in varying concentrations are well mixed with the solid, and the amount of solute removed is determined. The capacity of a solid to remove a solute is a function of the concentration of the solute. The results of the experiment are plotted on a graph that shows the solute concentration versus the amount sorbed onto the solid. If the sorptive process is rapid compared with the flow velocity, the solute will reach an equilibrium condition with the sorbed phase. This process can be described by an **equilibrium sorption isotherm.** It is an example of a sufficiently fast, heterogeneous surface reaction. If the sorptive process is slow compared with the rate of fluid flow in the porous media, the solute may not come to equilibrium with the sorbed phase, and a **kinetic sorption model** will be needed to describe the process. These are insufficiently fast, heterogeneous surface reactions. Travis and Etnier (1981) give a comprehensive review of sorption isotherms and kinetic models.

3.4 Equilibrium Surface Reactions

3.4.1 Linear Sorption Isotherm

If there is a direct, linear relationship between the amount of a solute sorbed onto solid, C^*, and the concentration of the solute, C, the adsorption isotherm of C as a function of C^* will plot as a straight line on graph paper (Figure 3.2). The resulting linear sorption isotherm is described by the equation

$$C^* = K_d C \tag{3.2}$$

The importance of using the hysteretic mode appears to be greater for the pressure head and the water content than for the pore velocity and the solute front movement.

4.11 Preferential Flowpaths in the Vadose Zone

The preceding analyses all treat the unsaturated zone as a homogeneous, porous medium. However, this is certainly not the case. In the root zone there are numerous large pores and cracks formed by such agents as plant roots, shrinkage cracks, and animal burrows. These **macropores** can form preferential pathways for the movement of water and solute, both vertically and horizontally through the root zone (Beven and Germann 1982). This situation can lead to "short-circuiting" of the infiltrating water as it moves through the macropores at a rate much greater than would be expected from the hydraulic conductivity of the soil matrix; see Figure 4.18(a).

A second type of preferential flow is **fingering,** which occurs when a uniformly infiltrating solute front is split into downward-reaching "fingers" due to instability caused by pore-scale permeability variations. Instability often occurs when an advancing wetting front reaches a boundary where a finer sediment overlies a coarser sediment, see Figure 4.18(b) (Hillel and Baker 1988).

A third type of preferential flow is **funneling** (Kung 1990b). Funneling occurs in the vadose zone below the root zone and is associated with stratified soil or sediment profiles. Sloping coarse-sand layers embedded in fine-sand layers can impede the downward infiltration of water. The sloping layer will collect the water like the sides of a funnel and direct the flow to the end of the layer, where it can again percolate vertically, but in a concentrated volume, as shown in Figure 4.18(c). Field studies using water containing dye placed in furrows indicate that the water is moving in the fine-sand layer above the discontinuity of the coarse-sand layer (Kung 1990a). These same dye studies showed that because of funneling, the volume of the soil containing dye decreased with depth. The dyed soil region occupied about 50% of the soil volume at 1.5 to 2.0 m; from 3.0 to 3.5 m, it occupied only 10% of the soil volume, and by 5.6 to 6.6 m, it was found in about 1% of the soil volume. At this depth a single column of dyed soil was found, obviously formed by funneling of flow of dyed water from above (Kung 1990a).

These occurrences of preferential flow in particular and soil heterogeneity in general have disturbing implications for monitoring solute movement in the unsaturated zone. Some studies have recorded seemingly anomalous results, with deeper soil layers having greater concentrations of solute than more shallow layers (Kung 1990b). These anomalies can be explained by preferential flow patterns, with infiltrating solute being directed to certain regions of the vadose zone by short circuiting, fingering, and funneling. This suggests that a large number of sampling devices in the vadose zone might be needed if a reasonably accurate picture of the distribution of a contaminant is to be obtained. As contaminants reaching the water table may need to pass through the unsaturated zone, preferential flow paths in the unsaturated zone also have implications for groundwater monitoring. In the case of a contaminant that was evenly spread on the land surface—for example, an agricultural chemical—one would expect that there would be an evenly distributed solute load reaching the water table via the vadose zone. However, due to preferential flow paths the mass of solute may be concentrated in some locations,

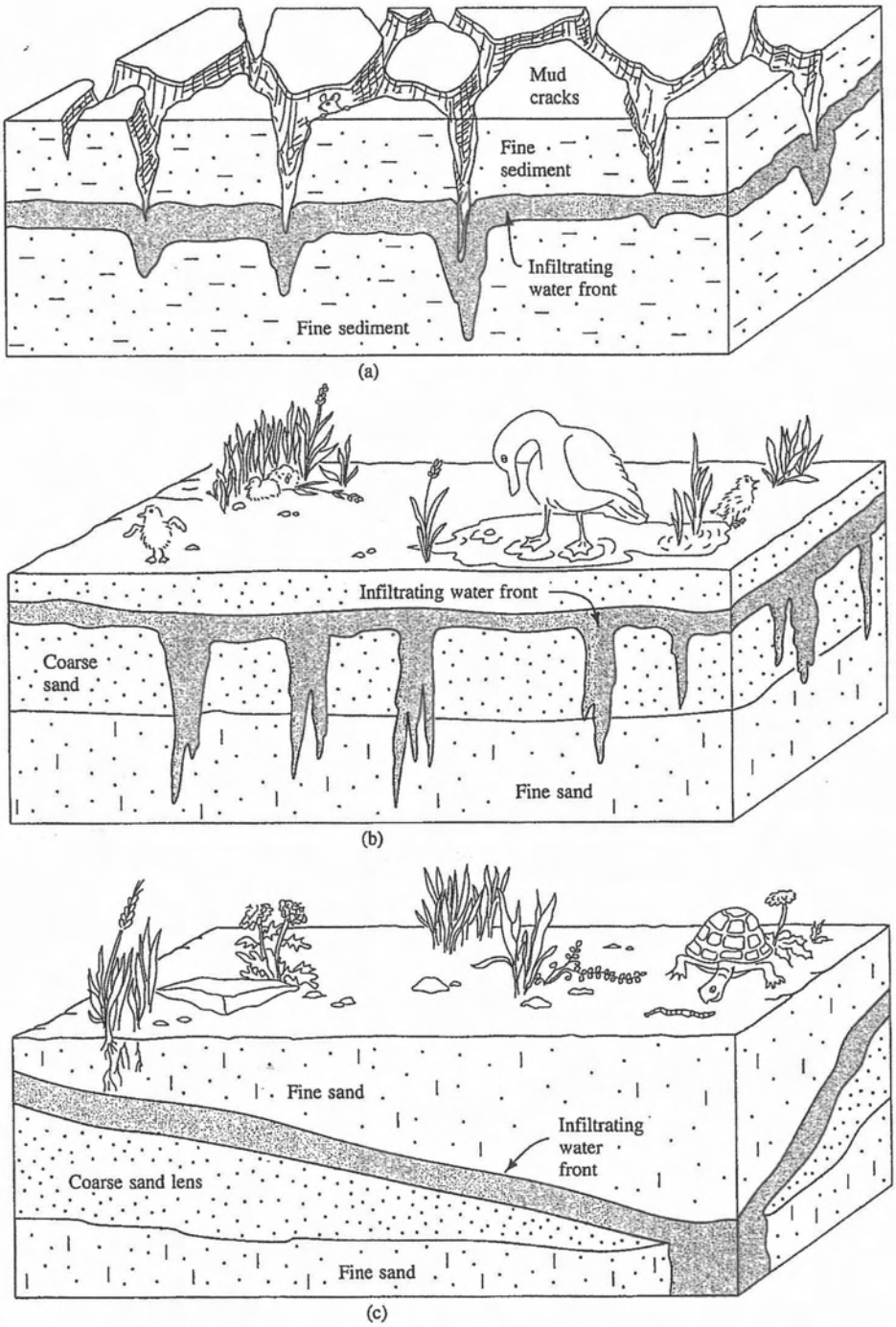

FIGURE 4.18 Preferential water movement in the vadose zone due to (a) short circuiting, (b) fingering, and (c) funneling.

resulting in an uneven distribution in the shallow ground water beneath the site. Monitoring wells beneath the site may show varying solute concentrations, depending upon how close they are to an up-gradient point of concentrated recharge.

4.12 Summary

The vadose zone extends from the land surface to the water table; moisture in the vadose zone is under tension. Soil particles can have charged surfaces, which can attract or repel anions and cations. Moisture moves through the vadose zone due to a potential that is the sum of the elevation potential and the matric potential. Matric potential is a function of the volumetric water content and depends upon whether the soil has previously undergone wetting or drying. The unsaturated hydraulic conductivity is also a function of the volumetric water content. The flux of moisture through the soil can be calculated from Darcy's law or the Buckingham flux law. The nonsteady flow of soil moisture is described by the Richards' equation. The nonsteady movement of soil vapor and soil moisture can also be described by a partial differential equation.

Solute movement through the vadose zone proceeds by both advection and diffusion. There is an advective-dispersive equation for solute transport in the vadose zone that accounts for retardation through sorption onto soil particles. Analytical solutions to this equation exist. Solute movement in the vadose zone is affected by regions of immobile water found in dead-end pores. It is also affected by an anion-exclusion zone when clays are present in the soil. Preferential pathways of solute movement may be present that create pathways for lateral movement of water in the vadose zone and concentrate infiltrating water into certain regions. Preferential pathways of water movement may make monitoring of the vadose zone and shallow water table difficult.

Chapter Notation

$A(z, t)$	Term defined by Equation 4.44
$B(z, t)$	Term defined by Equation 4.45
B_d	Bulk density of soil
C	Solute concentration
C^*	Solute phase bound to soil
C_i	Initial solute concentration in soil water
C_{im}	Solute concentration in immobile water
C_m	Solute concentration in mobile water
C_0	Solute concentration in injected water
C_{calc}	Concentration of solute calculated in soil if the water in the anion exclusion zone is included
D_v	Diffusion coefficient for water vapor
D^*_s	Soil-diffusion coefficient, which is a function of θ
D_s	Dispersion coefficient for soil moisture, which is a function of θ
D_{sm}	Dispersion coefficient for mobile soil moisture
e	Elementary charge of an ion

ENVIRONMENTAL SOIL PHYSICS

Daniel Hillel

Professor Emeritus
Plant, Soil, and Environmental Sciences
University of Massachusetts
Amherst, Massachusetts

With Contributions by
A.W. Warrick
R. S. Baker
C. Rosenzweig

ACADEMIC PRESS
San Diego London Boston New York Sydney Tokyo Toronto

in computing "average" animal size). However, assuming $\bar{v}$ to be a working approximation, we get

$$J_c = \bar{v}\theta c \tag{9.3}$$

It is sometimes useful to estimate the average *residence time* t_r of a solute within a layer of soil of thickness L (especially if we are concerned with a time-dependent interactive process, such as a chemical reaction, involving the solute under consideration). Accordingly,

$$t_r = L/\bar{v} \tag{9.4}$$

If the flow is impelled by gravity alone, that is to say if there are no pressure gradients, then the downward flux of liquid is equal to the hydraulic conductivity K of the medium, which in turn depends on its wetness θ:

$$q = K(\theta)$$

Using Eq. (9.2), we thus obtain for Eq. (9.4)

$$t_r = L\,\theta/K(\theta) \tag{9.5}$$

The foregoing equations allow us to estimate, for instance, the distance of travel of a soluble pollutant from the bottom of, say, a septic tank or sanitary landfill to the water table, through the so-called *unsaturated zone,* as follows:

$$L_t = t\,K(\theta)/\theta \tag{9.6}$$

where L_t is the average distance of convective transport in time t. If the values of wetness and hydraulic conductivity vary within the soil profile, as often happens, the foregoing calculations must be carried out layer by layer to determine the solution's space-variable flux, average distance of travel, and per-layer residence time.

A serious shortcoming in this approach is that we can seldom, if ever, assume that the transport of solutes occurs by convection alone. In reality, solutes do not merely move with the water as sedentary passengers in a train, but also move within the flowing water in response to concentration gradients in the twin processes of *diffusion* and *hydrodynamic dispersion.* Moreover, solutes are not always as inert as we have thus far assumed, since they tend to interact with the biological system within the soil (e.g., be taken up or released by microbes and the roots of higher plants) and with the physicochemical system (e.g., be adsorbed or exchanged by the soil's clay and humus fractions). Cations and anions are distributed differently in the soil solution. Cations are attracted to negatively charged mineral surfaces and hence are more prevalent at edges of pores, whereas anions are repelled by those surfaces and tend to be more prevalent toward the centers of pores. The flow rate being faster in the latter domains, anions tend to move ahead of cations in fine-grained soils. Additionally, solutes may undergo chemical reactions and may also be removed from solution by precipitation or volatilization. In other words, solutes resemble rather rowdy passengers who constantly move from car to car and occasionally jump off the train entirely while others jump on it.

conductivity increases in depth at a sufficient rate. In all the various instances of instability that Philip identified, it is essential that the flow be gravity assisted.

Parlange and Hill (1976) expanded their earlier work with a stability analysis that considers the velocity of the wetting front in relation to its curvature, as well as the influence of soil-water diffusivity on the propagation of a curved wetting front. This analysis repeated their earlier conclusion that fingers tend to develop if the frontal velocity is less than the saturated conductivity of the medium. Parlange and Hill conjectured that an increase in the initial wetness of the sublayer should induce an increase in the width of the developed fingers. Their theoretical approach was followed by a series of laboratory experiments by Glass *et al.* (1987, 1989).

An analysis by Hillel and Baker (1988) of infiltration into a layered profile, later tested by Baker and Hillel (1990), emphasized the potential importance of the *suction of water entry* (SWE) into an initially dry sublayer of higher permeability. This parameter had been ignored in previous treatments of unstable flow. Just as SWE determines the effective hydraulic conductivity of the sublayer, it also determines whether or not flow is accelerated with distance down the profile. When the wetting front reaches the interlayer boundary, it pauses until the suction there falls (or the pressure builds up) sufficiently to allow entry of water into the large pores of the sublayer. If at this point the conductivity of the sublayer exceeds that of the top layer, the sublayer cannot conduct throughout its entire volume, since it would then be conducting more water than it is receiving (an obvious impossibility). Hence the spatially distributed flow field with its parallel streamlines must begin to constrict at the critical depth (typically, at or just below the transition from the less permeable top layer to a more permeable sublayer), thus causing the streamlines to converge. In the case of a wide flow field, this forms spatially separated, partial-volume, flow paths (fingers).

In addition to explaining the phenomenon, the theory by Hillel and Baker (1988) also predicts the fractional cross-sectional area (F) of fingers that form under specified sets of conditions. In the general case,

$$F = [K_t/K_u(S_e)][(H_0 + Z_i + S_e)/Z_i] \tag{14.59}$$

Here K_t is the saturated hydraulic conductivity of the less permeable top layer, K_u is the unsaturated hydraulic conductivity of the sublayer (a function of the matric suction of water entry into the sublayer, S_e), H_0 is the hydraulic head imposed on the surface by the ponded water, and Z_i is the vertical thickness of the top layer (depth of the interlayer boundary below the soil surface).

In the extreme case where the sublayer is of very coarse texture whose water-entry value is effectively zero suction (i.e., a layer having such large pores or being so water repellent that it can only be penetrated by water under positive atmospheric pressure), and if the ponding depth at the surface is negligible, we get

$$F = K_{st}/K_{sb} \tag{14.60}$$

Thus, if the saturated conductivity of the sublayer is an order of magnitude (×10) greater than that of the top layer, then we may expect the fingers to

occupy some 10% of the cross-sectional area of the sublayer, and if it is two orders of magnitude greater, then the fingers will only occupy 1% of the soil volume. In such conditions detecting vadose zone fingering in the field by random sampling would be extremely difficult. (The hydrological term *vadose zone* refers to the entire volume of unsaturated but water-conducting domain—including the soil and the strata below it—that is above the water table. In other words, it is the *unsaturated zone* overlying the *saturated zone*.)

This estimation of the partial volume occupied by fingers ignores the lateral spread of water from the saturated core of each finger into the surrounding soil. This process, controlled by the soil's sorptivity, forms an unsaturated cylindrical sheath of moist soil around each finger. It is a relatively slow process, which, moreover, becomes progressively slower with time. If continued long enough, it may eventually moisten the entire sublayer but, because infiltration often occurs in brief episodes, the lateral sorption of water from the fingers is likely to be of limited importance during short-term infiltration.

Of particular importance is the effect of a sublayer's antecedent moisture on the pattern of infiltration and fingering. In principle, increasing the initial wetness of the sublayer can have a dual effect: (1) It reduces the suction gradient at the wetting front, thereby retarding infiltration during its transient phase, and (2) it may affect the water-entry suction, allowing sorption of water at a higher suction than if the soil were initially dry. The latter effect may be associated with the phenomenon of hysteresis, whereby the rewetting of a partially drained soil can occur at a higher suction than the entry of water into a completely dry soil. We may therefore conjecture that a higher antecedent sublayer wetness is likely to reduce the likelihood of a flux discrepancy between the layers, and hence to counter the tendency toward fingering and partial-volume flow. This reasoning also suggests that unstable flow is likely to be more prevalent in arid than in humid regions (Hillel, 1993).

Evidence from the field reveals that unstable flow is not merely a curiosity, of interest only to theoreticians and laboratory experimenters. Starr *et al.* (1978) studied the pattern of leaching in a layered soil consisting of a fine sandy loam overlying a coarse sand, with a water-table depth of 1.8 m. Removal of the soil layers following infiltration of a dye solution showed that most of the solution moved through fingers ranging from 0.05 to 0.2 m in diameter. In a second experiment, they applied a chloride solution to the soil surface and found that several salt pulses reached the water-table before the mean front had reached the 0.6-m depth. This greatly accelerated flow rate corresponded to the observations in the first experiment where flow was unstable and the solute moved in rapid fingers through the subsoil.

Preferential flow has important implications with regard to the movement of solutes in the soil (Germann *et al.*, 1984; van Genuchten *et al.*, 1984; Berkowitz *et al.* 1988; Steenhuis *et al.*, 1990). Hendrickx *et al.* (1988) conducted a bromide tracer trial in the Netherlands and found that, after 5 weeks with a total rainfall of 120 mm, the bromide concentration in the groundwater was 13 times higher when an unstable wetting front had formed than could be expected with a stable wetting front. In Wisconsin, Kung (1990)

found that water and solutes flowed through less than 10% of the soil volume at the 3.0- to 3.6-m depth layer.

OTHER FORMS OF PREFERENTIAL FLOW

The phenomenon of fingering is only one of several possible forms of *preferred pathway flow,* also known as *preferential flow,* in the soil. In contrast with the mode of *distributed flow,* in which water permeates the entire porous network of the soil matrix and moves through its entire volume, preferential flow occurs via distinct pathways that constitute only a fraction (sometimes only a small fraction) of the soil's total volume (Bouma, 1981; Gish and Shirmohammadi, 1991; Luxmoore and Ferrand, 1993).

Most readily evident are flow patterns that follow preexisting features in the soil profile such as clay or sand lenses, cavities, or fissures. The latter may either be formed physically by shrinking and cracking of clay, or formed biologically by burrowing animals (such as earthworms, ants, and rodents) or decaying roots. Finally, human manipulation of the land (including certain types of tillage such as subsoiling or chiseling) may form cracks that, in turn, constitute pathways for preferential flow.

A fairly common case is a clayey soil that shrinks on drying and forms cracks (or *macropores*) that begin at the surface and extend to some depth in the profile (Hoogmoed and Bouma, 1980). When such a soil is subsequently subjected to surface flooding or to a heavy downpour of rain, water under positive pressure immediately penetrates the cracks and quickly fills their volume, known as *macropore storage.* Thereafter, infiltration takes place from the water-filled cracks sideways into the soil blocks between the cracks, as well as downward from the bottoms of the cracks and from the soil surface (Fig. 14.12). The process is therefore multidimensional, and its pattern depends on the geometry of the cracks, the conductivity (or sorptivity) of the soil matrix, and the mode and duration of wetting (Beven and Germann, 1982; Edwards *et al.,* 1988).

During the initial period of infiltration, the intake rate of water by cracked soils can be extremely high (Mitchell and van Genuchten, 1991)—much

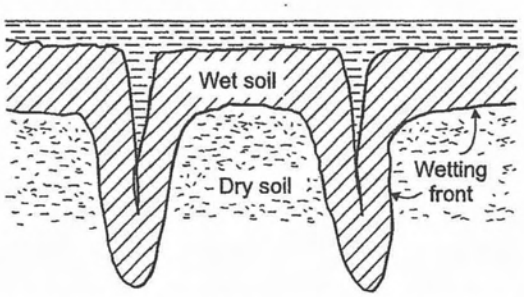

Fig. 14.12. Shape of the wetting front during ponded infiltration into a soil with open cracks.

higher than the saturated conductivity of the soil matrix (Fig. 14.13). However, if the infiltration process continues long enough, the influence of the surface cracks eventually diminishes, as the wetting front penetrates deeper into the profile well beyond the reach of the cracks, and as the cracks themselves tend to close due to the swelling of clay under prolonged imbibition.

A comprehensive discussion of the role of macropores in soil-water dynamics was published by Beven and Germann (1982). They pointed out that flow in the two domains (the macropores between soil blocks and the "micropores" within soil blocks) is governed by different potential gradients. They also showed that the sizes and the structures of the macropores determine the pattern of water flow. Accordingly, they classified macropores into four groups, on the basis of their morphology:

1. *Pores formed by burrowing animals* (e.g., worms, moles, gophers, armadilloes, or wombats): Such pores are usually tubular and may range in diameter from 1 mm to over 50 mm.
2. *Pores formed by plant roots:* These pores are also tubular, and their sizes and extensions depend on the type of plant. After the roots have decayed, these root channels remain for a time as hollow passages. Even in the case of living roots, preferential flow may take place along the soil–root interface (Gish and Jury, 1983).
3. *Cracks and fissures:* These are formed by shrinkage in clayey soils or by chemical weathering of the bedrock material. They may also be formed by freeze–thaw cycles and by such methods of cultivation as subsoiling.
4. *Natural soil "pipes":* These can form as a result of the erosive action of subsurface flows in highly permeable and relatively noncohesive soil materials when subjected to high hydraulic gradients.

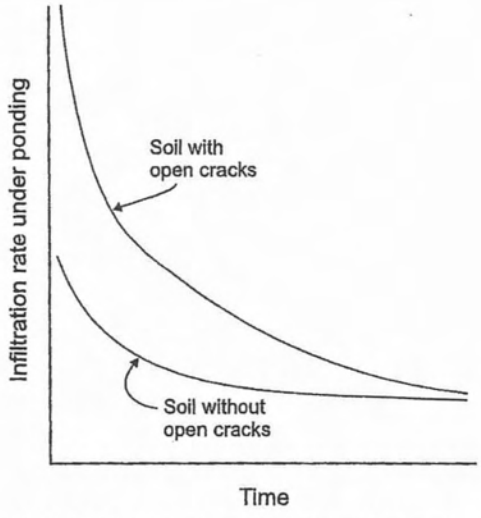

Fig. 14.13. Hypothetical infiltrability–time curves for a soil without and with open cracks.

Edwards *et al.* (1988) further clarified the influences of the size, frequency, vertical and lateral distribution, and continuity of macropores on the hydrological characteristics of soil profiles. They found that worm holes may extend to 1 m below the surface and can be quite durable.

Definitive work on infiltration in soils with macropores was done by Bouma (1981), Germann and Beven (1985), Beven and Clark (1986), Dagan (1986), and Shirmohammadi *et al.* (1991). Modeling studies were reported by Hoogmoed and Bouma (1980), Huyakorn *et al.* (1983, 1985), and Bruggeman and Mostaghimi (1991), among others.

The potential contribution of macropores to the process of infiltration can be assessed by comparing situations in which macropores conduct water to situations in which macropores are prevented from conducting water. The latter can be achieved by introducing the water to the soil surface at a suction rather than at a positive pressure. An instrument developed for this purpose is the disk infiltrometer, also called *suction* (or *tension*) *infiltrometer.* It is shown in Fig. 14.14 in comparison with the standard double-ring infiltrometer. The disk infiltrometer consists of a reservoir of water (usually designed to maintain a constant subatmospheric pressure by means of a Mariotte tube), at the bottom of which is fixed a porous plate. That plate introduces hydraulic resistance, and

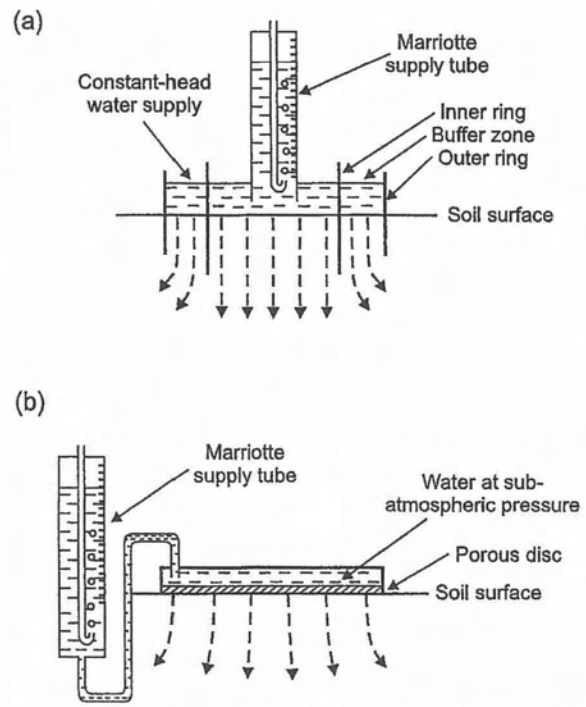

Fig. 14.14. Sectional view of two types of infiltrometers: (a) Conventional double-ring infiltrometer, supplying water to the soil surface at atmospheric pressure, (b) Disk infiltrometer, introducing water at subatmospheric pressure.

the hydraulic gradient through the plate when it is placed on the soil surface is such as to ensure a negative pressure (suction) at its contact plane with the soil. The suction thus imposed becomes a boundary condition for the infiltration of water into the soil (White and Perroux, 1987, 1989; Perroux and White, 1988; Elrick and Reynolds, 1992). A study of disk infiltrometers was carried out by Warrick (1992).

RAIN INFILTRATION

When rain or sprinkling intensity exceeds soil infiltrability, free water appears on the soil surface. In principle, the infiltration process should then be similar to the case of shallow ponding. If rain intensity is less than the initial infiltrability value of the soil but greater than the final value, then at first the soil will absorb at less than its potential rate and the flow of water in the soil will occur under unsaturated conditions; however, if the rain is continued at the same intensity, and as soil infiltrability declines, the soil surface will eventually become saturated. Thenceforth the process will continue as in the case of ponding infiltration. Finally, if rain intensity is at all times lower than the infiltrability, the soil will continue to absorb the water as fast as it is applied without ever attaining saturation. After a long time, as the suction gradients become negligible, the wetted profile will acquire a wetness for which the conductivity is equal to the water-supply rate, and the lower this rate, the lower the degree of saturation of the infiltrating profile. This effect is illustrated in Fig. 14.15.

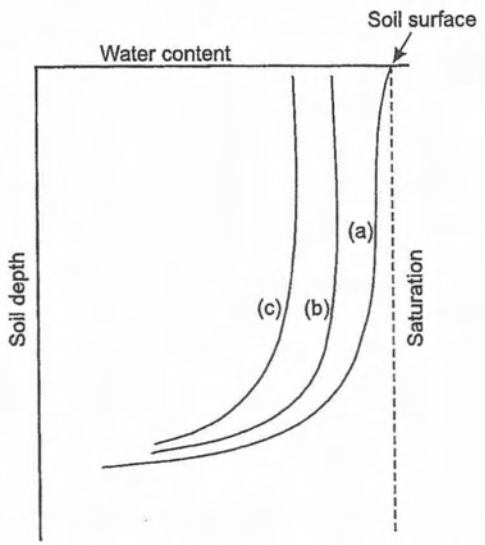

Fig. 14.15. The water-content distribution profile during infiltration (a) under ponding, (b) under sprinkling at relatively high intensity, and (c) under sprinkling at a very low intensity.

and conductivity of moist porous media. Soil Sci Soc. Am J. 43: 1050–1052.
Reece, Clive F., 1996. Evaluation of a line heat dissipation sensor for measuring soil matric potential. Soil Sci. Soc. Am. J. 60:1022–1028.
Riha, S.J., K.J. McInnes, S.W. Childs, and G.S. Campbell. 1980. A finite element calculation for determining thermal conductivity. Soil Sci. Soc. Am. J.44:1323–1325.
Shainberg, I., and H. Otoh. 1968. Size and shape of montmorillonite particles saturated with Na/Ka ions (inferred from viscosity and optical measurements). Isr. J. Chem. 6:251–259.
Tavman, I.H., 1996. Effective thermal conductivity of granular porous materials. Int. Commun. Heat Mass Transfer. 23(2):169–176.
Van Rooyen, M., and H.F. Winterkorn. 1959. Structural and textural influences on thermal conductivity of soils. p. 576–621. *In* Proc. Annu. Meeting 38th. Washington, DC. 5–9 Jan. 1959. Highway Res. Board, Natl. Res. Council, Washington, DC.
Van Wijk, W.R. (ed.). 1963. Physics of plant environment. North-Holland, Amsterdam.
Wierenga, P.J., D.R. Nielsen, and R.M. Hagan. 1969. Thermal properties of soil based upon field and laboratory measurements. Soil Sci. Soc. Am. Proc. 33:354–360.
Yadav, M.R., and G.S. Saxena. 1973. Effect of compaction and moisture content on specific heat and thermal capacity of soils. J. Indian Soc. Soil Sci. 21:129–132.

Impact of Preferential Flow on the Transport of Adsorbing and Non-Adsorbing Tracers

K.-J. S. Kung,* T. S. Steenhuis, E. J. Kladivko, T. J. Gish, G. Bubenzer, and C. S. Helling

ABSTRACT

Field experiments were conducted by using a tile drain monitoring facility to determine the impact of preferential flow on the transport of adsorbing and non-adsorbing tracers. Simulated rainfall with 7.5 mm h^{-1} intensity and 7.5 h duration was applied to a 18- by 65-m no-till plot. After 72 min of irrigation, a pulse of Br^- and rhodamine WT (water tracer) was applied through irrigation, and 4 h later, a second pulse of Cl^- and rhodamine WT was applied. The breakthrough curves (BTC) of these tracers were measured by sampling the tile. The same experiments were repeated in an adjacent conventional-till plot, except the rainfall intensity was reduced to 5 mm h^{-1}. The results showed that both the non-adsorbing and the adsorbing tracers applied in the same pulse arrived at the tile line at the same time and their BTC peaked at the same time. This suggested that water dynamics of preferential flow paths dominated the initial phase of the contaminant transport, regardless of the retardation properties of contaminants. The tracers from the second pulse were detected at only 13 min after application. Among the four tracer pulses in two plots, the BTC from the second pulse in the no-till plot had the longest period in which the non-adsorbing and adsorbing tracers had identical patterns. This indicated that the wetter the soil profile, the longer the water dynamics of preferential flow paths dominate the contaminant transport. The BTC from the second pulse applied to the two plots had identical arrival and peak times.

UNSATURATED SOILS have been thought to behave like a *living filter* system to protect groundwater quality; i.e., chemicals applied to the soil surface move slowly in unsaturated soils, are either taken up or strongly adsorbed, and are degraded to non-toxic compounds before leaching to groundwater. In laboratory experiments where soils were homogenized and repacked into columns, results showed that unsaturated soils could indeed filter out contaminants and purify water. This is why many highly toxic chemicals have been approved by regulatory agencies for agricultural use. However, results from field experiments have demonstrated that some agrichemicals could be rapidly transported downward in an unsaturated soil profile (Everts et al., 1989; Kladivko et al., 1991; Roth et al., 1991). The rapid contaminant transport in these studies was attributed to preferential flow. Helling and Gish (1991), Luxmoore (1991), Flury (1996), and Kladivko et al. (1999) summarized many research results from field experiments indicating that chemicals can be rapidly transported through certain pathways into the groundwater. Soil scientists have become increasingly aware of the importance of preferential flow as one of the most significant field-scale mechanisms to determine the pollution potential of chemicals. In essence, preferential paths make an unsaturated field soil behave like a perforated filter.

Among the three types of preferential flow paths, the in-situ scales, scope, and formation–destruction mechanisms of macropore flow paths are not yet clearly comprehended. Therefore, there is no evidence that impact of macropore flow on contaminant transport under field conditions can be accurately replicated and examined in laboratory studies. Consequently, the impact of macropore flow on contaminant leaching needs to be studied in field-scale experiments. The conventional sampling protocols (e.g., soil cores and solution lysimeters) used in field experiments to examine contaminant leaching were developed more than 50 years ago when the existence, mechanisms, and impacts of preferential flow were not understood. These sampling protocols implicitly assume that water-borne contaminants move through the entire soil profile. As a result, samples are collected at random locations and measured results are averaged. A sample collected near a preferential pathway will recover much more mass than those located away from a pathway. This partly explains why there was substantial scatter in sampling results that were based on the conventional sampling protocols (Ghodrati and Jury, 1992; Ju et al., 1997). When contaminants are transported through certain complex yet fixed pathways, sample locations rather than the number of samples determine the representativeness of the samples (Kung, 1990). The random samples collected by the coring method and the lysimeter method may significantly un-

K.-J.S. Kung, Dep. of Soil Science, and G. Bubenzer, Dep. of Biol. System Eng., Univ. of Wisconsin, Madison, WI 53706-1299; T.S. Steenhuis, Dep. of Agric. and Biological Eng., Cornell Univ., Ithaca, NY 14850; E.J. Kladivko, Dep. of Agronomy, Purdue Univ., West Lafayette, IN; T.J. Gish, Hydrology Lab., and C.S. Helling, Weed Science Lab., USDA-ARS, BARC-W, 10300 Baltimore Blvd., Beltsville, MD 20705-2350. Received 2 Feb. 1999. *Corresponding author (kung@calshp.cals.wisc.edu).

Published in Soil Sci. Soc. Am. J. 64:1290–1296 (2000).

Abbreviations: BTC, breakthrough curves; WT, water tracer.

derestimate solute breakthrough in soil with preferential flow paths. In order to accurately determine the impact of preferential flow on contaminant transport, one must first detect preferential pathways and then sample along the preferential pathways (Kung, 1990; Ju et al., 1997). However, there are no tools that can nondestructively and three-dimensionally map and visualize these complex macropore flow paths. Therefore, it is necessary to use an alternative sampling protocol to assess the total leaching.

Some agricultural fields are tile-drained to control the water table. If the tiles were installed with uniform spacing and depth, and border tiles were installed to partition the input area, a field above a tile will behave like a huge, enclosed and undisturbed lysimeter. As long as the watertable is above the tile line and vertical recharge into regional groundwater is negligible, contaminants leached down from a plot above a tile can be accurately and holistically assessed from tile flow, regardless of how rapid and localized the contaminants are being transported through preferential flow paths. Richards and Steenhuis (1988), Everts et al. (1989), and Kladivko et al. (1991) showed that their tile drain monitoring facilities can be used as an alternative sampling protocol to assess the impact of preferential flow on contaminant transport.

There are a number of factors that influence pesticide field behavior: soil hydraulic properties, soil clay and organic matter contents, hydro-geologic setting, and pesticide properties being the most critical (Cohen et al., 1986). Although direct comparisons of the relative importance of these factors were essentially non-existent, it has been shown that, within uniform soils without preferential flow paths, for a pesticide with low persistence, retardation had the greatest impact on its environmental fate (Gustafson, 1989). In field with preferential flow paths, Kladivko et al. (1991) co-applied three pesticides with different adsorbing properties and found that, after only 1 cm of net infiltration from natural precipitation occurred shortly after application, all pesticides were simultaneously detected in water samples collected from tile drains buried at 75 cm during the first day after the precipitation. One pore volume of the soil profile is ≈30 cm of water. This suggested that, shortly after application, pesticides with different adsorbing properties were equally susceptible to deep leaching through preferential flow paths.

Pesticide analysis is expensive and the total number of samples that can be collected and processed are often limited by the research budget. For this reason, non-adsorbing tracers such as bromide (Br^-) and chloride (Cl^-) and adsorbing tracers such as rhodamine WT dye and FD&C blue no. 1 dye have been frequently used among the published studies. Conventionally, it has been assumed that: (i) the breakthrough patterns of non-adsorbing tracers such as Br^- and Cl^- only represent the worst-case scenario of nitrate transport through preferential flow paths; and (ii) breakthrough patterns of adsorbing tracers such as dyes can simulate those of pesticides with retardation coefficients higher and solubility lower than those of Br^- and Cl^-. Everts et al. (1989) used adsorbing tracer rhodamine WT dye (with K_{oc} ranging from 1150–1650 mL g^{-1}) and non-adsorbing tracer Br^- to examine contaminant transport in simulated precipitations. By frequently sampling tile drain buried at 110 cm, they observed that both tracers had fast breakthrough patterns within the first four hour after the initiation of the irrigation. They also found that >80% of mass of the adsorbing tracer that leached out did so during the precipitation event. This confirmed that chemicals with different adsorbing properties were equally susceptible to deep leaching through preferential flow paths. The results also suggested that in order to accurately monitor the total mass of a contaminant leached out through preferential flow paths, it was critical to frequently sample during and shortly after a precipitation.

The initial soil water content can influence whether a chemical will be subject to deep leaching through preferential flow paths. The initial soil water content of Kladivko et al. (1991) was not determined, while that of Everts et al. (1989) was 0.34 $cm^3\ cm^{-3}$, which was the maximum water holding capacity. The objective of this study was to use a tile drain monitoring facility to compare the impact of preferential flow on the breakthrough time and pattern of both adsorbing (rhodamine WT) and non-adsorbing (Br^- and Cl^-) tracers uniformly applied to a soil surface for two different tillage practices under both initially dry and wet conditions.

MATERIALS AND METHODS

Field experiments were conducted at two plots of the Willsboro Research Farm of Cornell University in Willsboro, New York, in July 1996. Both plots were 18 m by 80 m and a tile was buried at ≈90-cm depth along the center of each plot over 15 years ago. The slope at the soil surface varies from 3 to 5%. A monitoring facility was installed in a manhole at the lower end of each plot to continuously measure the tile flow and periodically collect water samples. Plot 3 was under no-till continuous corn, while Plot 4 was under conventional till corn–soybean rotation. The Farm is along the west shore of Lake Champlain and the soil of the site is Rhinebeck variant loam (fine, illitic, mesic Aeric Epiaqualfs) originated from glacial outwash, which consists of five distinct layers: fine sandy loam (0–21 cm); clayey loam (21–42 cm); clayey hard pan (42–64 cm); gravely loam (64–99 cm); and gravely sand (>99 cm).

In order to use tile as an alternative sampling protocol, the watertable must be above the tile line. From previous records, the flow rate of tile drainage would decrease slowly from 100 to 10 mL s^{-1} after a rainfall and then quickly drop from 10 to 0 mL s^{-1}. Based on this information, the current experiments were conducted when the flow rate reached ≈5 mL s^{-1} and there was no precipitation in the 5-day weather forecast. A simulated rainfall with 7.5 mm h^{-1} intensity was applied to Plot 3 for 7.5 h by a solid set sprinkler system to simulate a spring shower. The irrigated area was 18 m by 65 m, which covered the entire width of the plot and was 5 m from the lower end of the plot. The riser height of the sprinkler head was 1.5 m and the height of corn was ≈1.0 m (there was an unprecedented amount of natural precipitation in early summer that postponed the experiments well past crop emergence.)

Shortly after the irrigation started, non-adsorbing tracer

KBr (15.3 kg Br^-) and adsorbing tracer rhodamine WT (0.65 L solution with 15% by weight) dissolved in 150 L water were injected into the irrigation water at the pump, which was located ≈1.6 km (about a mile) from the plots. By visually observing the color of the irrigation water at the sprinkler nozzles, it was found that the first pulse of tracers arrived at the plot between 72 min and 96 min after the irrigation started. About 4 h after injecting the first pulse of tracers, KCl (19.6 kg Cl^-) and rhodamine WT (0.65 L solution with 15% by weight) were again dissolved in 150 L water and injected into the irrigation water at the pump. This pulse of tracers arrived at the plot between 311 min and 335 min after the irrigation started.

The first pulse was to test the impact of preferential flow on the transport of non-adsorbing and adsorbing tracers under relatively drier soil conditions, while the second pulse was to test under wetter conditions. Identical experiments were also conducted in Plot 4, except the irrigation intensity was reduced to 5 mm h^{-1} for 7.5 h to reduce surface runoff. There was no facility to measure the water and chemicals lost in surface runoff. Furthermore, fewer tracers were applied in Plot 4; i.e., 8.27 kg Br^- and 0.35 L rhodamine WT with 15% by weight were applied in the first pulse, and 12.7 kg Cl^- and 0.35 L rhodamine WT with 15% by weight were applied in the second pulse. The timing and method of the tracer application in Plot 4 were identical to those in Plot 3.

During the first 12 h after the irrigation started, water samples were collected from the tile every 6 min. From 12 to 18 h, water samples were collected every 15 min. From 18 to 24 h, water samples were collected every 30 min. During the second and the third days, water samples were collected every 2 h. The samples were stored at approximately 5°C until analyzed, except during a short period of shipping. Flow rate of the tile drain was continuously measured during the 3-d period by the tipping-bucket method. The Br^-, Cl^-, and nitrate in the water samples were analyzed using the method discussed in Kung et al. (2000), while rhodamine WT was analyzed by using fluorolite fluorescent meter with 425 nm excitation and 515 nm reflection filters. The detection limits of Br^-, Cl^-, and nitrate were 0.25, 0.5, and 0.5 mg L^{-1}, respectively, while that of the rhodamine WT was 1 μg L^{-1}.

RESULTS AND DISCUSSION

Based on measurement from 18 rain gauges, the irrigation in Plot 3 had Christianson uniformity of 0.89 (corn plants within 1.5 m of each rain gauge were removed). The tracer BTC and tile hydrograph from Plot 3 are shown in Fig. 1. The tile flow started to increase quickly at 52 min after irrigation started. Soil has a spectrum of pores. As water enters into unsaturated soil, the gradient of matric potential will favor water to first fill the smaller matrix pores. As the small pores are filled, the gradient of matric potential diminishes quickly and water will start to move down through some of the larger structural pores that constitute the preferential flow paths. The fast water arrival and the quick increase of tile flow may be caused by either *old matrix water* being pushed out from the soil profile, or by *new irrigation water* moving down through the preferential flow paths. The background concentrations of the Cl^- and nitrate in the tile drainage before irrigation began were 31 and 54 mg L^{-1}, respectively. These two chemicals were from previous fertilizer application and were stored in soil matrix pores in the unsaturated soil profile. Extra Cl^- was applied through irrigation water (the concentration of Cl^- from water samples taken from Lake Champlain at the inlet of water pump was 12 mg L^{-1}). Figure 1 shows that the concentrations of the Cl^- and nitrate from tile drain actually decrease gradually when tile flow increases quickly. If the initial tile flow were caused by the old matrix water, the concentrations of the Cl^- and nitrate should have been steady. Because the irrigation water from Lake Champlain had relatively less Cl^- and no nitrate, the background concentrations of the Cl^- and nitrate contributed from soil matrix pores were diluted by the newly applied and cleaner irrigation water as tile flow increased. This suggested that some water from irrigation had bypassed the soil matrix pores and moved down quickly to watertable through preferential flow paths.

The background concentrations of the Br^- and rhodamine WT in tile flow were below detection limits. Both Br^- and rhodamine WT were first detected from the water sample collected at 96 min after the irrigation started (or 24 min after the application). The measured saturated hydraulic conductivities of the different layers in this site were in the range of 0.5 to 5 × 10^{-6} m s^{-1}. If there were no preferential flow, it would have taken ≈2 d for the applied tracers to arrive at the tile line under a free drainage condition with unit gradient (i.e., $v = q/\theta = 7.5$ mm $h^{-1}/0.4 = 18.9$ mm h^{-1} and $t = L/v = 0.9$ m/18.9 mm $h^{-1} \approx 2$ d). Because samples were taken once every 6 min, whether the adsorbing tracer rhodamine WT had the exact same arrival time as that of the non-adsorbing tracer Br^- was unknown (i.e., it was possible that one tracer arrived earlier than the other between adjacent sampling interval). Nevertheless, it was not expected that a highly adsorbing tracer like rhodamine WT arrived at a tile buried at 0.9-m depth at only 24 min after its application. In short, the rapid arrival time unambiguously demonstrated that preferential flow dictates the initial transport of an adsorbing contaminant.

It has been conventionally conceptualized that water enters into preferential flow paths such as macropores only when the soil surface is very wet (i.e., soil surface was nearly saturated with localized ponding). The gravimetric water content of the top 30 cm of soil, based on 9 cores taken from an adjacent area before the irrigation started, was between 11 and 15%, while the saturated water content of the soil was 36%. About 15 mm irrigation water was applied during the first 2 h and this was far from enough to saturate the top 30 cm soil. According to our visual observation, there was neither localized ponding nor surface runoff during the first two hours after irrigation started. The first pulse of tracers arrived at the plot between 72 min and 96 min after the irrigation started. This indicated that contaminant transport through preferential flow paths occurred when the top 30 cm soil was under unsaturated conditions.

Figure 1 also shows that the BTC of both Br^- and rhodamine WT reach a peak at the identical time (i.e., 126 min after the irrigation started or 54 min after tracer application). From the arrival to the peak of the tracers applied in the first pulse, tile flow increased very quickly

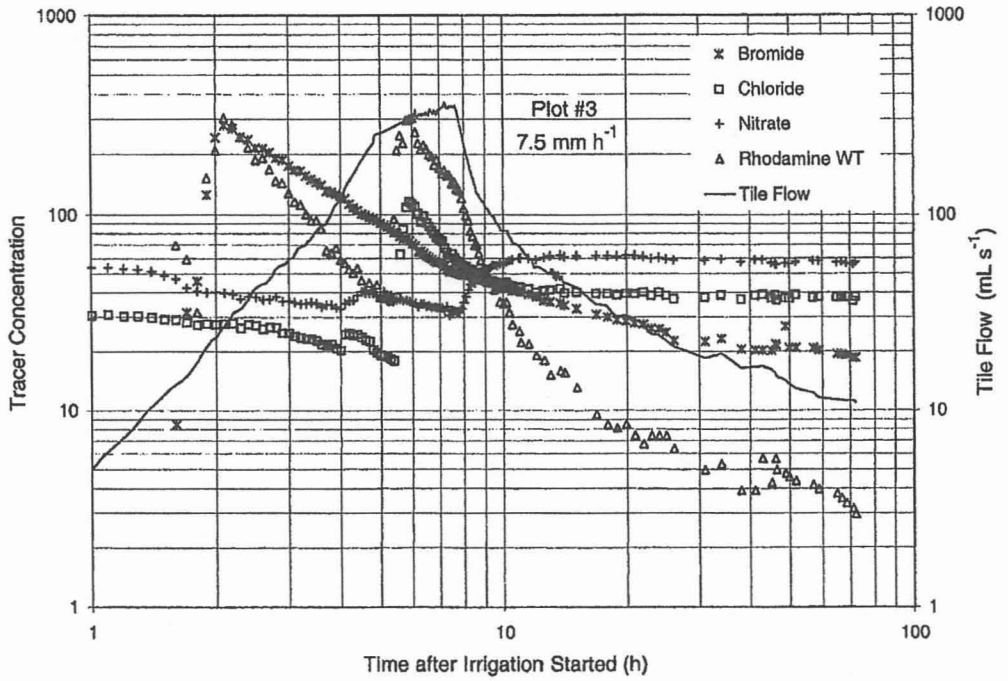

Fig. 1. The breakthrough curves of the non-adsorbing and adsorbing tracers and the tile hydrograph from Plot 3 as function of time after the irrigation started. The concentration is in mg L^{-1}, except that of rhodamine WT is in $\mu g\ L^{-1}$.

and the concentrations of both Cl^- and nitrate continuously decreased. This suggested that more and more preferential flow paths became hydraulically active. As an adsorptive tracer transported down through a preferential flow path, it was expected that some would be retarded along the wall of the path. For this reason, it has been conventionally assumed that because Br^- have essentially no retardation effect, they represent the worst-case scenario of contaminant transport through preferential flow paths. However, the similarity of the initial BTC of the Br^- and rhodamine WT suggested that an adsorbing tracer was as susceptible to fast and deep leaching through preferential flow paths as the non-adsorbing tracers. This indicated that the chemical properties of the tracer had less effect on the initial transport through preferential flow paths.

As shown in Fig. 1, the Cl^- and rhodamine WT applied in the second pulse again arrived at the tile drain at the same time (i.e., 324 min after irrigation began or 13 min after tracer application). The BTC of these two chemicals had similar shape and peaked at the same time (354 min after irrigation began or 43 min after application). This fast breakthrough confirmed that it was the water dynamics, instead of the chemical properties of the tracer, that dictated the initial transport of contaminants through preferential flow paths. The rate of tile flow at the time of the Cl^- arrival was about 10 times higher than that at Br^- arrival. This suggested that many more preferential flow paths had became hydraulically active. The fact that the Cl^- arrival time was much shorter than that of Br^- suggested that the newly hydraulically active preferential flow paths had either larger pores or straighter paths. When a soil profile becomes wet, because the matric potential gradient decreases, it is logical that preferential flow paths with larger pores would become hydraulically active. There is no reason that a straighter preferential flow path would became hydraulically active later than a more tortuous path with identical equivalent pore radius. Therefore, the shorter arrival time was probably because some Cl^- was transported through preferential flow paths with larger pores, which were not hydraulically active earlier.

Figure 1 also shows that the BTC of the Br^- and rhodamine WT have similar patterns during the first 36 min after initial arrival at the tile drain, while those of Cl^- and rhodamine WT have almost the identical shape during the first 140 min after initial arrival. This indicated that, the wetter the soil profile, the more tracers had entered into preferential flow paths with larger pores and, hence, the longer the transport of an adsorptive tracer will behave like that of a non-adsorptive tracer. This confirmed that (i) the preferential flow paths had a spectrum of pore sizes and that (ii) some preferential flow paths with larger pores were initially not hydraulically active when their soil profile was dry.

When comparing the tails of the BTC of the adsorbing and non-adsorbing tracers applied in both pulses, it was clear that the adsorbing tracer rhodamine WT trailed off much more quickly. The tracers arriving at the tile early must be transported through the preferential paths with the larger pores. An adsorbing tracer that entered into preferential flow paths with larger pores would have less residence time in the unsaturated zone and a higher probability to reach the watertable without being adsorbed. On the other hand, tracers arriving at the tile

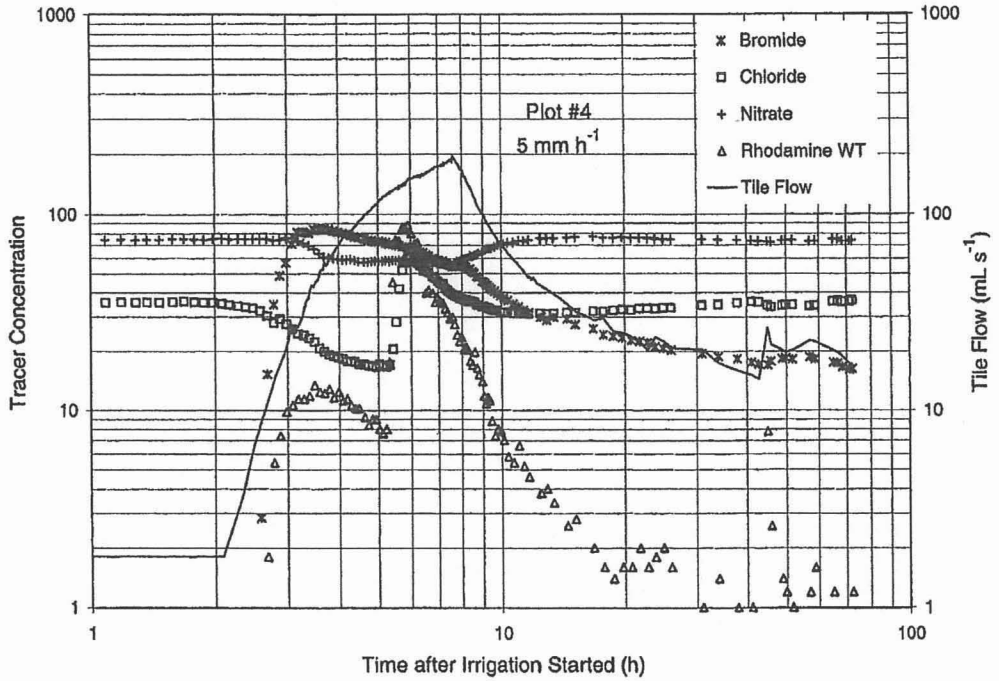

Fig. 2. The breakthrough curves of the tracers and the tile hydrograph from Plot 4. The concentration is in mg L^{-1}, except that of rhodamine WT is in μg L^{-1}.

at the tail of the BTC were transported either through the preferential paths with the smaller and/or more tortuous preferential pores or through soil matrix pores. Within the smaller and/or more tortuous pores, an adsorbing contaminant would stay in soil longer and have a higher probability of being retarded. As a result, the chemical adsorption would play a more important role in determining the total deep leaching when a contaminant is transported through smaller and/or more tortuous pores. Under an extreme case, where soil is homogenized and repacked in a laboratory column to destroy preferential flow paths, the fast breakthrough would be eliminated and the chemical properties of the contaminant would completely dominate the transport. These results were consistent with the fate of five pesticides (with different retardation factors) in field experiments by Gish et al. (1990).

The tracer concentrations and tile hydrograph from Plot 4 are shown in Fig. 2. Tile flow started to quickly increase at 140 min after irrigation. The background concentrations of the Br^- and rhodamine WT from the tile flow were below their detection limits, while those of the Cl^- and nitrate were 36 and 75 mg L^{-1}, respectively. Again, the concentrations of the Cl^- and nitrate decreased initially by dilution, as those shown in Plot 3. The later water arrival in Plot 4 was mainly because the irrigation intensity in Plot 3 was 50% higher (5 mm h^{-1} in Plot 4 and 7.5 mm h^{-1} in Plot 3). Bromide and rhodamine WT were detected from the water sample collected at 162 and 168 min after the simulated rainfall started (or 90 and 96 min after the application of the first pulse of tracers), respectively. These arrival times were slower as compared to that in Plot 3 (24 min after tracer application). Because the irrigation intensity in Plot 3 was 50% higher, the surface soil in Plot 3 was wetter when the first pulse of tracers was applied, and hence the tracers in Plot 3 had a greater chance to enter and be transported quickly through preferential flow paths.

The Cl^- and rhodamine WT applied to Plot 4 in the second pulse arrived at the tile drain at 324 min after irrigation started (or 13 min after tracer application), which was exactly the same as that in Plot 3. This confirmed that more preferential flow paths with larger pores became hydraulically active when a soil profile became wetter. Furthermore, the BTC of the Cl^- and rhodamine WT peaked at 354 min after irrigation started (or 43 min after tracer application), which was again exactly the same as that in Plot 3. This suggested that, as a soil profile became wetter, the larger end of the pore spectrum of the hydraulically active preferential flow paths in Plots 3 and 4 became similar. These results were not expected because the Plot 3 was under no-till continuous corn, while the Plot 4 was under conventional tillage with corn–soybean rotation. Nevertheless, the BTC of Cl^- and rhodamine WT in Plot 4 started to trail off earlier than those in Plot 3. This was probably because the soil profile in Plot 3 was wetter when the second pulse of tracers was applied, and the larger end of the pore spectrum of the preferential flow paths in Plot 3 was hydraulically active longer.

Because less water and tracers were applied to Plot 4, the peak of the tile hydrograph, as well as the peak concentrations of the tracers shown in Fig. 2, are lower than those in Fig. 1. In Fig. 1, the two peaks of the rhodamine WT have almost identical concentration. In

Fig. 2, however, the first peak of the rhodamine WT has a much lower concentration than that of the second peak. Within each plot, the total amount of rhodamine WT applied in the two pulses was identical. Among the four pulses of tracer applications in two plots, the least amount of irrigation water (6 mm) was applied when the tracers from the first pulse in Plot 4 were applied. As a result, the adsorbing rhodamine WT from the first pulse applied to Plot 4 had a higher probability of entering smaller pores and being retarded.

Figures 1 and 2 show that as the tile flow starts to decrease, the concentrations of the rhodamine WT decrease quickly by two orders of magnitude. From tracer concentration and tile flow, mass flux of the leached tracer can be calculated. The result showed that, of the total mass leached out from the tile, >90% of rhodamine WT was leached during the first 20 h. This suggests that the vast majority of the deep leaching of absorptive pesticides occurs during the first day after a precipitation event. Currently, there is no guideline on when and how frequently to collect samples in the coring and lysimeter sampling protocols. Results from this study confirmed the observation by Everts et al., (1989) that, in order to accurately assess the deep leaching of adsorbing pesticides, one must intensively sample during the first day after a major precipitation event.

The mass recoveries of Br^- from tile flow in Plots 3 and 4 were 3.41 and 3.51% of the total mass injected into the irrigation water at the irrigation pump, respectively; while those of rhodamine WT were 0.79 and 0.194%, respectively. Note that the real mass recoveries were unknown because: (i) the pipeline from the lake to the site was ≈1.6 km long and there were several leakage spots along the joints and vents; (ii) some tracers left the plots through surface runoff, which occurred at about 4 and 5.4 h after irrigation started in Plots 3 and 4, respectively; and (iii) the corn canopy was ≈1 m in height and unavoidably intercepted some of the tracers applied. Therefore, although the exact amount of each tracer injected into the irrigation water was known, the exact amount of mass actually infiltrated into the soil surface could not be accurately estimated. Furthermore, some tracers that reached the water table probably had flowed within the saturated zone and drained toward the adjacent bordering tiles, which were not monitored. Nevertheless, it was clear that much more nonadsorbing tracer leached out than the adsorbing tracer. This was mainly because the tail of the adsorbing tracer trailed off much more quickly. The total mass recoveries of Cl^- were not calculated because the soil profile had high initial Cl^- concentration. It was impossible to partition the newly applied Cl^- from the old Cl^- in the soil.

CONCLUSIONS

The impact of preferential flow on the transport of adsorptive and non-adsorptive chemicals was examined in field experiments. General results showed that both non-adsorbing and adsorbing tracers arrived at the tile quickly and their BTC peaked at the same time. This suggested that preferential flow dictated the initial phase of the transport, regardless of the retardation properties of the chemicals. As a soil profile became wetter, more tracers were transported through preferential flow paths and the water dynamics of preferential flow paths dominated the contaminant transport for a longer time. Specific results were:

1. In no-till Plot 3 with 7.5 mm h^{-1} irrigation, tile flow started to increase at 52 min after irrigation, while both tracers from the first pulse arrived at the tile in 24 min after their application. In conventional-till Plot 4 with 5 mm h^{-1} irrigation, tile flow increased at 140 min after irrigation, and non-adsorbing and adsorbing tracers from the first pulse arrived at 90 min and 96 min after application, respectively. The fast arrival of the tracers and the continuous dilution of the nitrate and Cl^- concentrations in tile flow demonstrated that some water and tracers bypassed the bulk soil matrix and arrived at the watertable quickly through preferential flow paths.
2. All tracers applied in the second pulse to both plots arrived at only 13 min after application. This indicated that preferential flow paths had a spectrum of pore sizes and more and more preferential flow paths with larger pores became hydraulically active as the soil profile became wetter. The fact that tracer breakthrough from the second pulse applied to the two plots had identical arrival times suggested that, as the soil profile became wetter, the larger end of pore spectrum of the hydraulically active preferential flow paths in the no-till and conventional-till plots became similar.
3. The BTC of non-adsorbing and adsorbing tracers from the first and second pulses peaked at the same time in both plots. This suggested that, regardless of the chemical retardation properties, the initial phase of the contaminant transport was completely dictated by the water dynamics of the preferential flow paths.
4. The tail of the BTC of the adsorbing rhodamine WT tracer always trailed off much more quickly than those of the non-adsorbing tracers. This indicated that, when an adsorptive contaminant was transported through the smaller and/or more tortuous pores, the chemical properties played a more important role in determining the transport.

ACKNOWLEDGMENTS

Research supported by the USDA-NRICGP grant 96-35102-3773. The views and conclusions contained in this document are those of the authors and should not be interpreted as representing the official policies, either expressed or implied, of the U.S. government.

REFERENCES

Cohen, S.Z., C. Eiden, and M.N. Lorber. 1986. p. 170–196. *In* W.Y. Garrner et al. (ed.) Evaluation of pesticides in groundwater. Symp. Ser. 315. Am. Chem. Soc., Washington, DC.

Everts, C.J., R.S. Kanwar, E.C. Alexander, Jr., and S.C. Alexander. 1989. Comparison of tracer mobilities under laboratory and field conditions. J. Environ. Qual. 18:491–498.

Deep vadose zone hydrology demonstrates fate of nitrate in eastern San Joaquin Valley

Thomas Harter
Yuksel S. Onsoy
Katrin Heeren
Michelle Denton
Gary Weissmann
Jan W. Hopmans
William R. Horwath

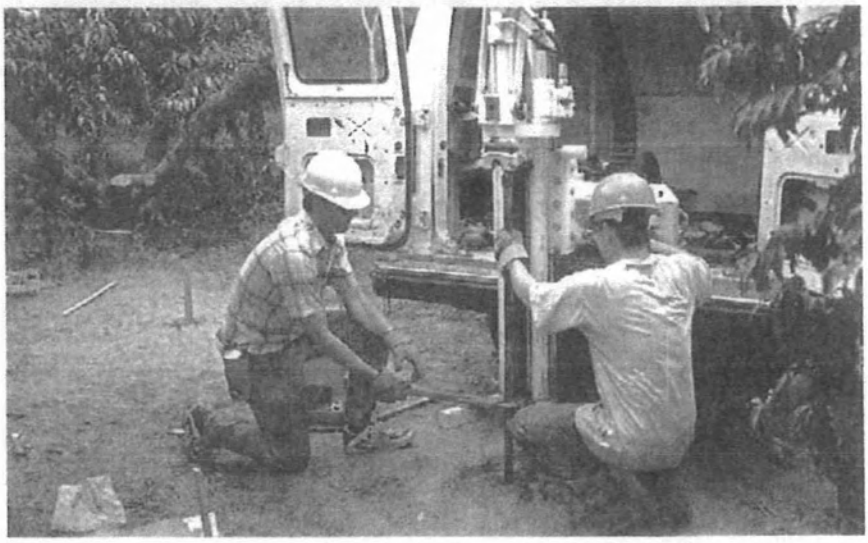

Nearly 3,000 feet of continuous soil cores were obtained between July and October 1997 using the Geoprobe direct-push drilling method. This method allowed for complete recovery of undisturbed cores throughout the 52-foot deep vadose zone. *Above*, UC Davis vadose zone hydrology professor Jan Hopmans (left) and Fresno State geology undergraduate Anthony Cole operate the coring equipment.

The sustainability of water resources is key to continued prosperity in the San Joaquin Valley and California. The vadose zone is an often-ignored layer of wet but unsaturated sediments between the land surface and the water table. It plays an important role in groundwater recharge and in controlling the flux and attenuation of nitrate and other potential groundwater contaminants. In a former orchard at the UC Kearney Research and Extension Center, we investigated the processes that control the movement of water, nitrate and other contaminants through the deep vadose zone. These processes were found to be controlled by the alluvial sedimentary geology of the vadose zone, which is highly heterogeneous. This heterogeneity should be considered when interpreting soil and deep vadose zone monitoring data and assessing of the leaching potential of agricultural chemicals. The transport of contaminants through the vadose zone may be significantly faster than previously assumed, while denitrification is likely limited or insignificant in the oxic, alluvial vadose zone of the eastern San Joaquin Valley.

For decades, the leaching of agricultural chemicals (fertilizer, especially nitrate, and pesticides) has been a concern of agronomists, soil scientists and hydrologists. Federal legislation first recognized the potential impacts to water resources in the early 1970s, when the Clean Water Act, the Safe Drinking Water Act, the Federal Insecticide, Fungicide, and Rodenticide Act and other legislation related to water pollution were enacted. Since then, countless efforts have been mounted by both the scientific-technical community and the agricultural industry to better understand the role of agricultural practices in determining the fate of fertilizer and pesticides in watersheds (including groundwater) and to improve agricultural management accordingly.

Much of the scientific work related to subsurface nitrate and pesticide leaching has focused on two areas: documenting the extent of contamination in groundwater; and investigating the fate of these chemicals in the soil root zone (including the potential for groundwater leaching) as it relates to particular agricultural crops and management practices. Rarely are these two research areas linked within a single study.

In California's valleys and basins, particularly in Central and Southern California, groundwater levels are frequently much deeper than 10 feet (3 meters) and sometimes as deep as 150 feet (45 meters) or more. Hydrologists refer to the unsaturated zone above the water table as the vadose zone. In general, only the uppermost 4 to 6 feet (1 to 2 meters) is described in soil surveys and investigated in soil studies; the deep vadose zone below the root zone remains largely outside the area of research and regulatory activity.

Yet, the vadose zone below the root zone stores significant moisture. All water and contaminant transport from the land surface to groundwater passes downward through the vadose zone. Few studies have investigated the fate or potential fate of, for example, nitrate and other contaminants in such deep vadose zones. Key questions include, What is the time of travel through the deep vadose zone? And, is there significant denitrification (natural attenuation) of nitrate in the deep vadose zone?

Pioneering work on nitrate in deep soil profiles was presented by Pratt et al. (1972) who investigated nitrate profiles in a Southern California citrus orchard to depths of 100 feet (30 meters); they estimated that it would take between 10 and 50 years for nitrate to leach to that depth. Average nitrate-nitrogen levels

Preferential flow paths, which are responsible for most of the water and solute transport from the root zone to the water table, quickly flush nitrogen to deeper portions of the vadose zone and to the water table, allowing for little or no denitrification.

below the root zone varied from 15 to 35 milligrams per liter (mg/L) under a 50 pounds per acre (lb/ac) treatment and from 35 to 55 mg/L under an excessive 350 lb/ac treatment. Based on gross mass-balance estimates, denitrification at that site was estimated to account for up to 50% of nitrate losses in the thick unsaturated zone profile where application rates were high.

Lund et al. (1974), supported later by Gilliam et al. (1978), Klein and Bradford (1979) and Rees et al. (1995), argued that nitrate losses in the deep vadose zone (due to denitrification) were strongly correlated with the textural properties of the soil. High losses were found in soils with pans or textural discontinuities, while losses were limited in relatively homogeneous, well-draining soils in other areas of Southern California. In contrast, Rolston et al. (1996), using isotope analysis at sites in the southern Sacramento Valley and the Salinas Valley, found little evidence of significant denitrification, even in thick unsaturated zones.

To study deep unsaturated zone hydrology, we established a research site in a former 'Fantasia' nectarine orchard at the UC Kearney Research and Extension Center (KREC) in Fresno County. The objective of our work is to provide a comprehensive assessment of the fate of nitrate in a 52-foot (16-meter) deep alluvial vadose zone that is typical of many agricultural areas in California. The assessment included detailed geologic, hydraulic and geochemical characterization, using nitrate as an example.

Field sampling

A 12-year fertilizer management experiment (from 1982 to 1995) was implemented in a 'Fantasia' nectarine orchard (Johnson et al. 1995). The fertilization experiment consisted of five application treatments in a random block design with triple replicates. Treatments included annual nitrogen application rates ranging from 0 to 325 pounds per acre (0 to 365 kilograms per hectare [kg/ha])(fig. 1). For the vadose zone characterization, three treatment subplots (0, 100 and 325 pounds per acre) were selected in 1997 (2 years after termination of the experiment), which we refer to as the control, standard and high subplot, respectively.

To start, we conducted a conventional root-zone nitrogen (N) mass-balance analysis from application and harvest records for the 12-year experiment in the three subplots. The analysis showed that the annual nitrogen leaching of excess nitrogen fertilizer from the root zone into the deep vadose zone was 51 (± 19), 83 (± 30) and 245 (± 42) pounds per acre. Water losses from the root zone to the deep vadose zone in the flood-irrigated orchard amounted to 1,100 (± 180) millimeters

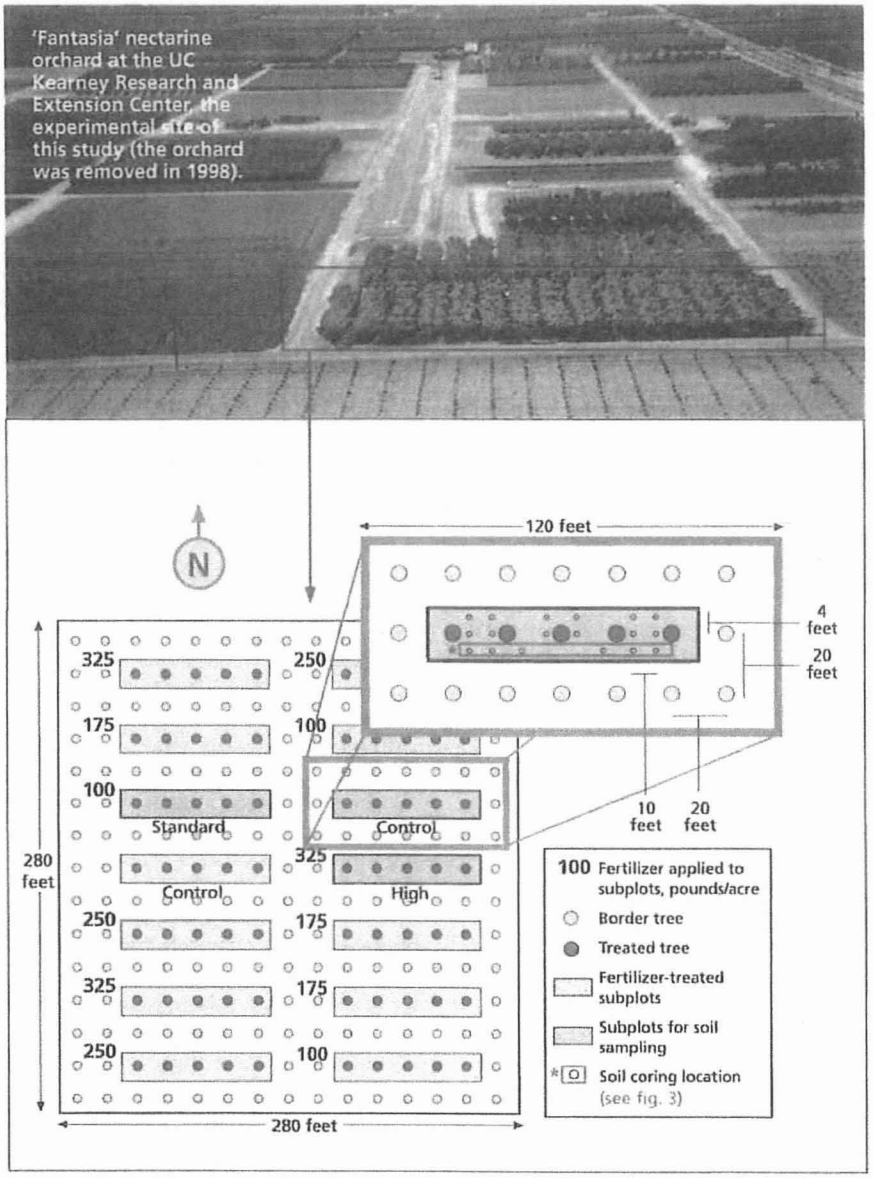

Fig. 1. In 1997, extensive core drilling was conducted, 2 years after the completion of three orchard nitrate-management trials at KREC with annual fertilizer rates of 0, 100 and 325 pounds nitrogen per acre. The complete random block design of the management trial and the three subplots selected for the deep vadose zone drilling are shown.

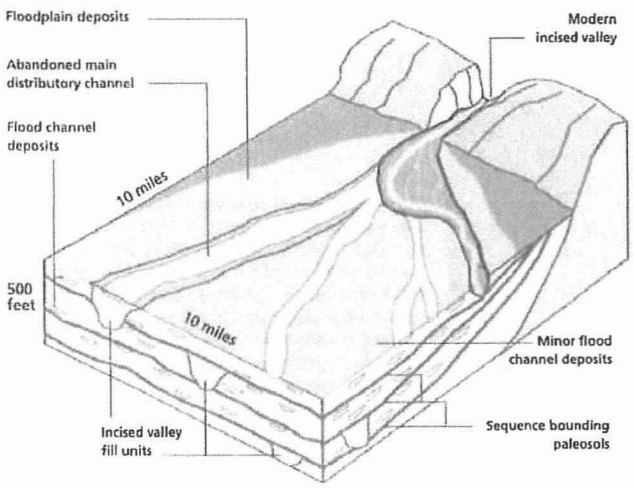

Fig. 2. Schematic diagram of the Kings River alluvial fan and its geologic elements.

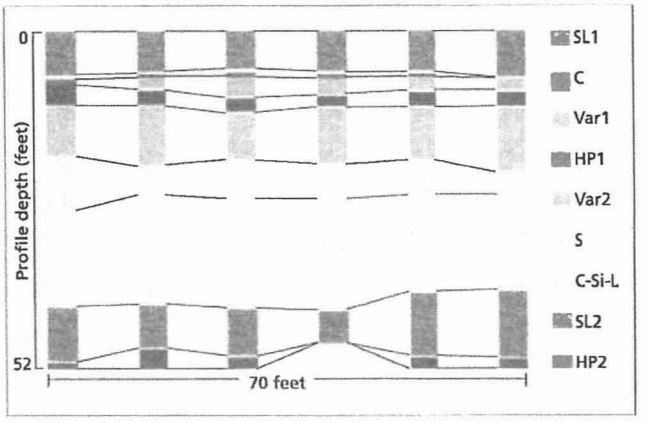

Fig. 3. The 10 major lithofacies identified at the two east-west cross sections, 140 and 144 feet from the southern edge of the orchard. The lithofacies, classified in the field according to color, texture and cementation, exhibit vertically varying thicknesses, yet are laterally continuous over the experimental site. Sandy loam is the most frequent textural unit, while clay is the least.

per year (Onsoy et al. 2005). Assuming uniform flow conditions throughout the deep vadose zone at an average soil moisture content of 25%, the travel time through the deep vadose zone was projected to be 3.2 (± 0.5) years. Based on the leaching rate and travel time, and taking into account that the experiment ended 1 year prior to drilling, we estimate that the deep vadose zone nitrogen storage at the time of drilling would be on the order of 195, 233 and 426 pounds nitrogen per acre in the control, standard and high subplot, respectively.

To confirm this estimate and to determine the applicability of the uniform flow concept, 60 undisturbed sediment cores were obtained in 1997 by drilling to the water table at a depth of 52 feet (16 meters) using a Geoprobe direct-push drilling technique. After geologic characterization of the complete core sections, 1,200 samples were collected (approximately one every 2.5 feet [0.8 meters]). Samples were collected for each sedimentologic stratum or substratum. The soil samples were preserved and stored for later analysis of their texture, hydraulic properties (water content, unsaturated hydraulic conductivity and water retention functions) and biochemical properties (pH, dissolved organic carbon, nitrate-nitrogen, ^{15}N isotope analysis).

Geologic framework

The site is located on the Kings River alluvial fan, approximately 2 miles (3.2 kilometers) west of the current river channel. The quaternary alluvial sediments (that is, sediments deposited by a stream) are derived exclusively from the hard, crystalline Sierran bedrock. Stratigraphically, the quaternary deposits in this part of the valley can be divided into five units (Marchand and Allwardt 1981): the post-Modesto (youngest), Modesto, Riverbank, Upper and Lower Turlock Lake deposits. Except for the post-Modesto, which is less than 10,000 years old (Holocene), these deposits are of Pleistocene age (2 million to 10,000 years old).

Most of the stratigraphic units (sediment facies) found at the site are believed to represent separate alluvial episodes related to several Sierran glaciations. In cores from the study site, these deposits appear as intercalated, thick and thin lenses of clayey silt, silt, sand and gravel from fluvial deposition. Channel sediments consist of moderately to well-sorted, subangular to subrounded sand and gravel. These channel deposits are surrounded by muddy sand and silts of floodplain deposits (fig. 2)(Page and LeBlanc 1969; Huntington 1980; Weissmann et al. 2002). Deposits from the various periods of Sierran glaciations are vertically separated by paleosols. Paleosols are buried soil horizons that were formed on stable upper-fan or terrace surfaces during interglacial periods, when no sediment deposition took place (fig. 3).

The vadose zone sediments are most easily classified by their texture, which ranges from clay to small gravel and includes a wide spectrum of predominantly silty to sandy sediments. The colors of the sediments range from grayish brown to yellowish brown, and more randomly to strong brown (no significant reduction zones). The thickness of individual beds varies from less than 0.4 inch (1 centimeter) for some finely layered clayey floodplain deposits to more than 8 feet (2.5 meters) for sandy streambed deposits. Sharp as well as gradual vertical transitions are present between texturally different units. The relative proportion of the five major textural categories found in the sediment cores was 17.2% sand, 47.8% sandy loam, 13.8% silt loam/loam, 8.3% clay loam/clay and 12.9% paleosol (see sidebars, pages 128 and 129; fig. 4).

KEY (figs. 3, 4): The major lithofacies are:

- SL1 — **recent Hanford sandy loam**
- C — **clay, very thin**
- Var1 — **variable sedimentary structures, predominantly sand**
- HP1 — **shallow paleosol (hardpan), red**
- Var2 — **various textures, sandy loam to clay loam**
- S — **medium sand**
- C-Si-L — **clay/clayey silt/clay loam, fine-textured floodplain deposits**
- SL2 — **sandy loam and**
- HP2 — **deep clayey paleosol (hardpan), red**

Hydraulic properties variability

Hydraulic properties of the unsaturated zone, such as the hydraulic con-

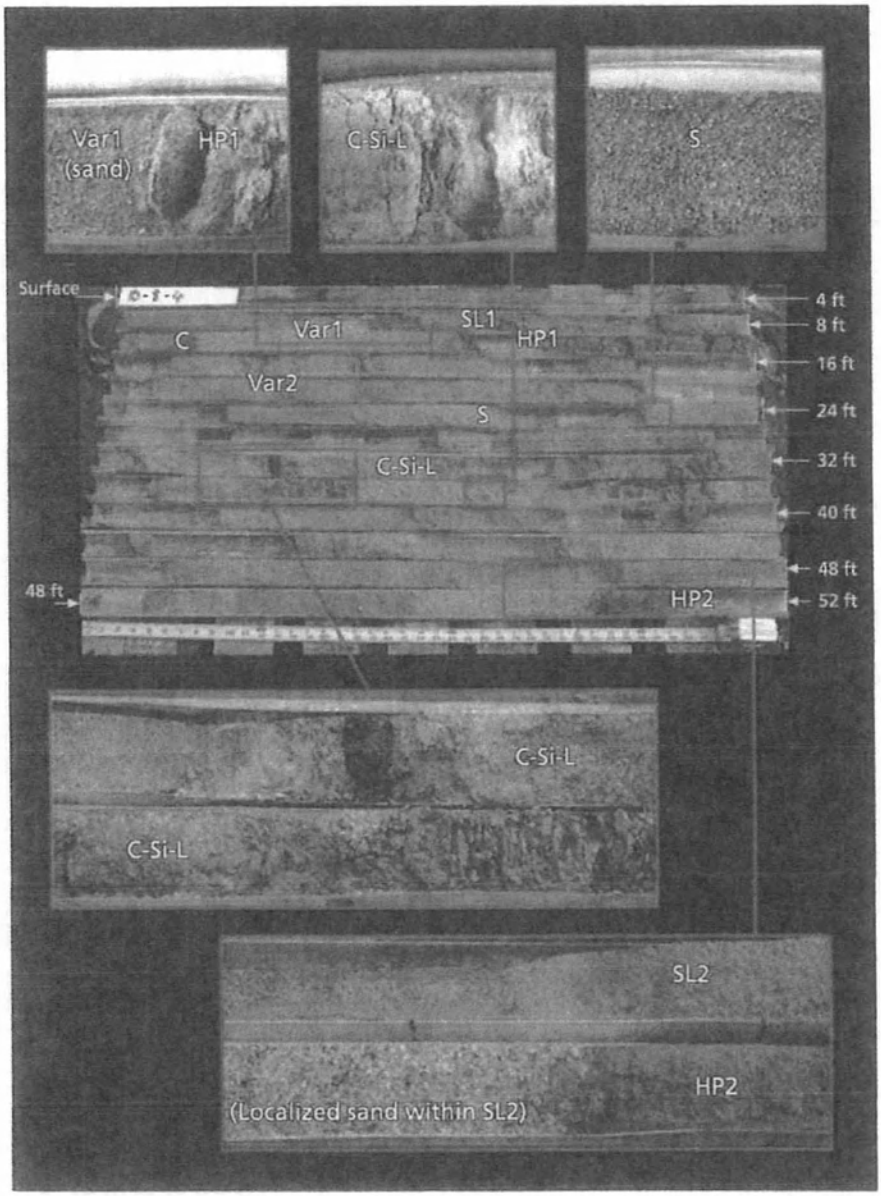

Fig. 4. Individual core sections were collected in 4-foot (1.2 meter) plastic tubes (see fig. 1). This image shows all 13 sections of a 52-foot (15.6-meter) core, lined up from the ground surface (*upper left*) to the bottom of the core (*lower right*). Missing subsections represent soil sampling locations for hydraulic and chemical analysis.

ductivity / moisture curve and the water retention curve — and the spatial distribution of these properties — strongly control the flow of water and the transport of nitrate and other solutes in the deep vadose zone. (Hydraulic conductivity is a measure of how fast water can percolate through the sediments; the higher the moisture and the coarser the sediments, the higher the hydraulic conductivity.) Hydraulic properties were determined in the laboratory on more than 100 undisturbed sediment core samples (3.5 inches [9 centimeters] long by 1.5 inches [3.8 centimeters] diameter) taken from various locations and depths at the orchard site. The laboratory tests involved measuring the water percolation rates in each core at six to 10 different moisture conditions, then determining the hydraulic properties by computer analysis.

Given the large amount of textural variability observed in the cores, it was not surprising that we found the hydraulic properties to also vary significantly, both with depth and laterally across the site (Minasny et al. 2003). The saturated hydraulic conductivity, for example, varied over nearly four orders of magnitude. Within some sedimentary layers (facies) we observed nearly as much hydraulic variability within individual facies as between facies. By far the highest conductivity was observed in sandy facies ("S" and "Var1" in figs. 3 and 4).

Heterogeneity of water flow

Traditionally, water flow between the root zone (at depths of 6.6 feet ([0 to 2 meters]) and the water table (here a depth of 52.8 feet [16 meters]) has been considered essentially a uniform, vertically downward flow process in a more or less homogeneous vadose zone. Within this conceptual framework, water from individual rainfall or irrigation events is thought to be initially stored in the root zone. There, it is available for uptake by the roots. Surplus water then gradually drains into the deeper vadose zone. Individual rainfall or irrigation events create pulses of moisture that penetrate the root zone profile. Through root water uptake and vertical spreading, the moisture pulse dampens out as it travels downward. In the deeper portions of the vadose zone, the downward flow rate has therefore been thought to be equal to the annual recharge rate.

However, the highly heterogeneous geology of the alluvial sediments observed at the orchard site, coupled with the associated heterogeneity of the hydraulic properties, suggest that this traditional conceptual framework is inadequate to describe how water and chemicals are transported through the vadose zone to the water table. Using our field data and computer simulation, we reconstructed two-dimensional cross-sections of the vadose zone that reasonably reflect the spatial variability

Major facies in the study-site vadose zone

The **sand** ("S" and "Var1") is quartz-rich, and contains feldspar, muscovite, biotite, hornblende and lithic fragments consistent with the granitic Sierran source (see figs. 3 and 4). Cross-bedding at the scale of few inches (centimeters) could be observed in some fine-grained sand samples. The dominant color of the sand is a light gray to light brown, the brown hue increasing with increasing loam content. The thickness of the sand beds is as much as 8 feet (2.4 meters), though thickness varies across the study site. Very coarse sand and particles up to pebble grain-size (up to 0.4 inch or 1 centimeter) could occasionally be observed at the bottom of the sand units, but were not present in all the cores. The sand units typically show a subtle fining-upward succession. The basal contact is typically sharp. The texture and distribution of these sandy deposits are consistent with deposition in a fluvial distributary channel on the Kings River fluvial fan. One ancient river channel was observed in cores collected from the orchard site, and it appears to have had a northeast-southwest orientation. The mean thickness of this channel deposit is nearly 6 feet (1.7 meters). The basal coarse sand and pebbles probably represent channel lag deposits that were laid down in deeper parts of the channels.

Sandy loam ("SL1," "SL2") is the most frequent lithofacies within the profile. The color is usually light olive to yellowish brown. Some of the sandy loam sediments are considered to be weakly developed paleosols because of their stronger brownish color, root traces and presence of aggregates. Mean bed thickness is 20 inches (50 centimeters), though individual beds can be as much as 7 feet (2 meters) thick. The sorting is moderate to good. Clay flasers and thin (fractions of an inch, 0.5 to 1 centimeter) clay laminae occur in some sandy loam units. Sandy loam sediments are assumed to have developed at the edge of channels, as levee or as proximal floodplain deposits near the channels.

Silt loam, loam and silty clay loam (portions of "C-Si-L" and "Var2") are usually slight olive brown to brownish gray in color. The bed thickness is within a range of a few inches to a foot (centimeters to decimeters). Fine-grained sediments often show sharp contacts between the units. Changes from one unit to the next exist on small distances. Lamination can more frequently be observed within silty sediments than in fine sands. Root traces and rusty brown–colored mottles are quite common. The depositional environment was presumably the proximal to distal floodplain of the fluvial fan, an area dissected by distributary streams.

The finest sediments are grouped in the fourth category: **silt, clay and clay loam** (portions of "C," "C-Si-L" and "Var2"). These are believed to have been deposited in the distal floodplain and in ponds that developed in abandoned channels. The main color is brownish gray to olive brown. Fine, less than 1-millimeter-diameter root traces and rusty brown mottles are common in the clay sediments. Statistics for the thickness of clay layers in the unit between 27 and 43 feet (8 and 13 meters) depth show a mean thickness of 5 inches (12.8 centimeters), but the mode is about 2.2 inches (3 centimeters). A 20-inch (50-centimeters) thick clay bed was observed at approximately 8 feet (2.5 meters) depth in most of the cores.

Paleosols ("HP1," "HP2") were recognized in different stages of maturity. They show a brown to strong brown, slightly reddish color, exhibit aggregates, ferric nodules and concretions, few calcareous nodules and hard, cemented layers. They also display a sharp upper and a gradual lower boundary as is typical for paleosols (Retallack 1990). Clay content decreases downward in the paleosols. Another feature is fine root traces, though these are typically obliterated in the more mature paleosols. Paleosols formed in periods of stasis marked by nonerosion and nondeposition, during the interglacials (Weissmann et al. 2002). The thickness of the paleosol horizons ranges from 20 inches (50 centimeters) to about 7 feet (2 meters).

of the hydraulic properties observed in the field, then we simulated water flow through this reconstructed vadose zone. Figure 5 illustrates the spatial distribution of the water flux through a hypothetical cross-section at 40 feet, similar to that observed at the orchard site. It captures important features that are characteristic of water flow in heterogeneous vadose zones (Russo et al. 1998; Harter and Yeh 1996). Understanding that flow occurs in this highly irregular pattern is important for interpreting the field data.

In particular, figure 5 shows that even though the simulated water application at the surface was uniform, the heterogeneity of the vadose zone forces water into distinct preferential flow paths (warm colors), separated by large areas of relatively stagnant flow (cooler colors). The preferential flow paths have highly irregular shapes, but are continuous and extend to the water table. The preferential flow paths occupy only a small portion of the vadose zone. In contrast, areas with relatively stagnant water flow occupy most of the vadose zone. Soil moisture differences between these two zones are small. Soil moisture is therefore not a particularly sensitive indicator and may not be useful for identifying the presence and location of these preferential flow paths.

In our study, further field work and computer simulations indicate that the location of these preferential flow paths does not change over time, even though they may partially or completely dry out between infiltration events. A new event will recreate the same set of preferential flow paths.

Preferential flow paths are not only created by the sediment heterogeneity. Other conditions may also trigger and support preferential flow paths: macropores in the root zone; flow instability during infiltration into sand or loamy sand soils (Wang et al. 2003); flow through or above embedded clay or sand lenses ("funneling")(Kung 1990); and "fingering" as a result of a sharp textural boundary within the vadose zone where the finer-textured (silt/clay) layer is located above a coarse-textured (sand) layer (Glass and Yarrington 2003).

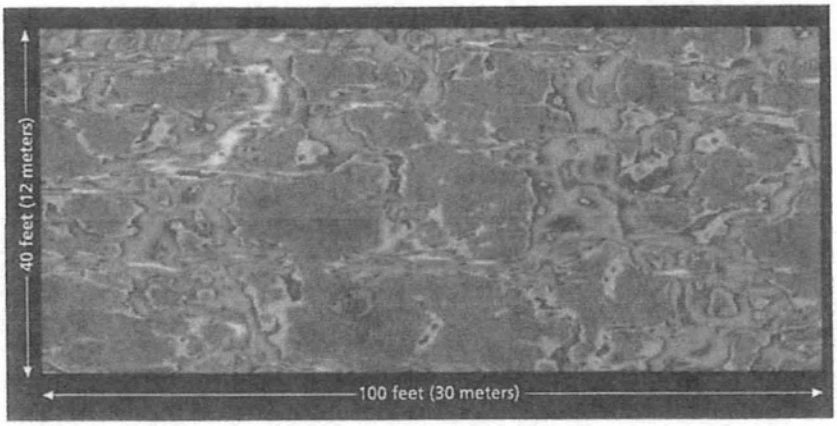

Fig. 5. Hypothetical, computer-simulated, unsaturated water flow rates through a heterogeneous vadose zone, illustrating how heterogeneity in the unsaturated zone generates preferential flow paths: Warmer colors (red, orange, yellow) represent high flow rates, and cooler colors (blue, violet, black) represent lower flow rates. The unsaturated hydraulic properties used for the simulation are similar to those found at the KREC research site.

Since much of the annual recharge occurs through these preferential flow paths, the actual downward flow rate is locally much higher than that estimated when assuming that the entire vadose zone uniformly participated in the downward water flow. Hence, solute travel times through deep vadose zones are likely shorter than if flow were indeed uniform. Because of the shorter travel time, nitrogen storage in the deep vadose zone should be significantly lower than estimated based on the uniform flow concept. On the other hand, under heterogeneous conditions, relatively old water may be trapped in the more stagnant portions of the vadose zone for extended periods. Do the measured nitrate distribution and water chemistry in the deep vadose zone at the Kearney site support this alternative conceptual framework of water and solute flow through the vadose zone?

Nitrogen distribution

To address this question, nitrate-nitrogen (NO_3-N) concentrations were measured in 809 subsamples of our cores. We found that the data were indeed highly variable and log-normally distributed (the logarithms of the data were normally distributed). Nitrate-nitrogen concentrations ranged from less than the detection limit of 0.05 milligram per liter (mg/L)(224 samples or 28% of the sample population) to more than 100 mg/L (two samples). Approximately 10% of the samples exceeded the maximum contamination level for drinking water (10 mg/L), set by the U.S. Environmental Protection Agency under the Safe Drinking Water Act. More than half of those occurred in the subplot with the highest nitrogen application. Mean nitrate-nitrogen concentrations (not including nondetects) in the control, standard and high subplot vadose zone were estimated to be 5.2, 3.3 and 7.4 mg/L, respectively (Onsoy et al. 2005). The nitrate-nitrogen coefficient of variation (CV) ranged from 1.6 to 2.4 within each subplot. The difference between the control and standard subplots was statistically not significant due to the large variability. But the high subplot yielded significantly larger mean nitrate-nitrogen concentrations throughout the profile, consistent with the overapplication of fertilizer.

Within all three subplots, slightly higher nitrate-nitrogen levels were observed in the root zone than in the deep vadose zone below the root zone, possibly due to the last fertilizer application in fall 1996, prior to our drilling. Other than that, we observed no significant vertical nitrate-nitrogen trend in the deep vadose zone.

The highest number of nondetects occurred in the coarse-textured, sandy lithofacies and in the sand lithofacies (above historic water level). There, approximately half of the samples had nondetectable nitrate-nitrogen levels. This is consistent with findings that fingering or preferential flow is particularly dominant in sandy unsaturated sediments. In other words, much of the sand facies does not participate in the flow (stagnant moisture) and would see little or none of the nitrate-nitrogen that is passing through the preferential flow paths.

Study-site geologic profile

A number of distinct sedimentologic units are recognized in the vadose zone profile throughout the orchard and are used to construct a field-scale geologic framework for the research site (see figs. 3 and 4).

The deepest parts of the cores (between 50 and 52 feet [15 and 15.8 meters]) display a strong brownish-colored, clay-rich paleosol. This paleosol marks the top of the upper Turlock Lake deposits (Weissmann 2002). Directly above this paleosol, from depths between 40 and 50 feet (12 to 15 meters) below the surface, the main textural units are sandy loam to fine sandy loam, with some coarse sand and gravel or fine-grained sediments. In the cores with fine sediment at the bottom of this unit, a coarsening-upward succession was observed in this zone; in the other cores a fining-upward cycle was observed.

Between 27 and 40 feet (8 and 12 meters) depth, the sediments are vertically and laterally quite heterogeneous with relatively thin bedding (thickness of a few inches [centimeters] to a couple of feet [few decimeters]), consisting mainly of clayey, silty and loamy material. Another strong brownish paleosol occurs at a depth of 30 to 33 feet (9 to 10 meters). Between 20 and 30 feet (6 and 9 meters) below the surface, a distinct sand layer, representing a former stream channel bed, is found. This unit has laterally varying thickness averaging nearly 6 feet (1.7 meters). A weak, mostly eroded paleosol was developed on top of the sand unit.

From about 10 to 13 feet (3 to 4 meters) to 20 feet (6 meters) below the surface, sandy loam with intercalated sand, clayey and silty material is found. Different trends of upward-fining and upward-coarsening are found on top of each other and laterally next to each other within this unit.

Immediately above the unit, at a depth of about 10 to 13 feet (3 to 4 meters), a nearly foot thick (0.2 meter) to more than 10 feet (1 meter) thick paleosol hardpan occurs. This paleosol marks the top of the Riverbank formation. Recent ground-penetrating radar surveys indicate that this paleosol is laterally extensive across the orchard site.

Sandy loam and subordinated loamy sand and loam are present from the top of the paleosol to the surface, and represent the Modesto deposits at the site. About 8 feet (2.5 meters) below the surface, a laterally continuous clay horizon with a thickness of few inches (centimeters) is found in most of the cores.

Most importantly, the total nitrogen mass estimated directly from the measured nitrate-nitrogen distribution in the deep vadose zone was only 46 (± 9), 37 (± 6) and 83 (± 12) pounds per acre annually for the control, standard and high subplots, respectively. This is less than one-quarter of the total nitrogen mass in the deep vadose zone that was indirectly estimated from the mass balance described above, which is based on the conventional uniform flow concept.

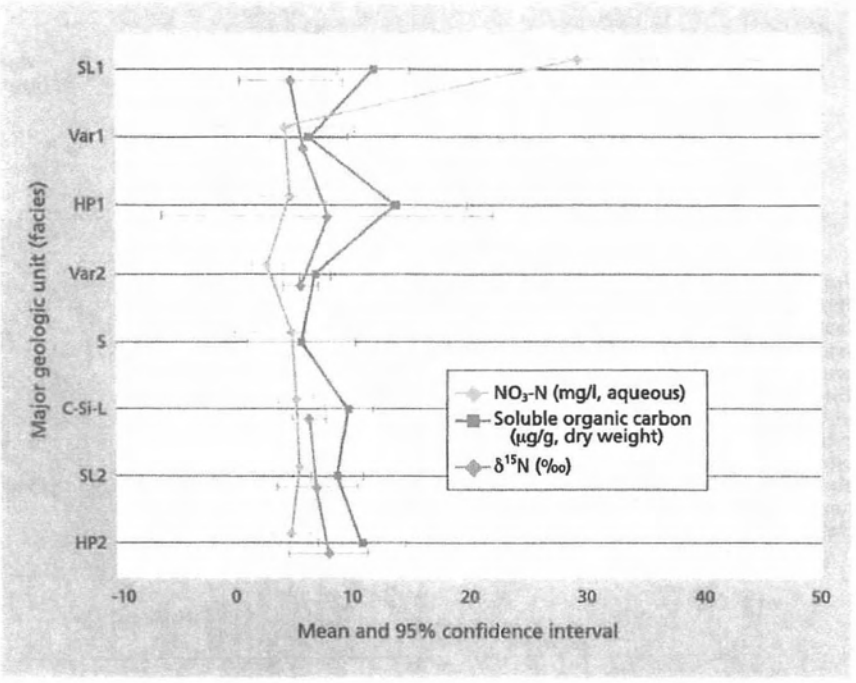

Fig. 6. Composite nitrate-nitrogen, dissolved organic carbon (DOC) and $\delta^{15}N$ profiles from borings at the orchard study site. Higher DOC indicates a higher potential for denitrification. Higher $\delta^{15}N$ levels (above 10) indicate the occurrence of partial denitrification.

Role of denitrification

Traditionally, such low nitrate-nitrogen mass in the deep vadose zone has been attributed to denitrification (the microbial breakdown process of nitrate by soil microbes). However, the lack of a significant vertical trend in the average nitrate-nitrogen concentration does not support that hypothesis (denitrification in the deep vadose zone would create a nitrate-nitrogen profile that shows decreasing concentration with depth). To further evaluate whether denitrification played a significant role in the deep vadose zone, we measured the amount of soluble organic carbon (a microbial food source) and the amount of $\delta^{15}N$ (a rare nitrogen isotope that increases in relative abundance when denitrification occurs) in the nitrate-nitrogen of samples from four cores (three from the high subplot and one from the standard subplot). (The concentration of isotopes is not reported in absolute values, but rather as a relative concentration, hence the notation "delta" or "δ" ^{15}N. A value of $\delta^{15}N$ = 5‰ indicates that the ^{15}N concentration is 5 permil above normal [1 permil = 0.1 percent].)

Soluble carbon was found to be very low, not favoring high rates of microbial degradation anywhere in the vadose zone profile. The $\delta^{15}N$ values varied from 0‰ to 12‰ and averaged 6‰ (fig. 6). Without denitrification, $\delta^{15}N$ levels are expected to be in the range of –5‰ to 5‰ (Rolston et al. 1996). Denitrification decreases nitrate-nitrogen concentrations, but increases the relative amount of isotopically heavy NO_3– $\delta^{15}N$. Indeed, there was a very weak trend ($R^2 < 0.1$) to support the hypothesis that a limited amount of denitrification may occur in the vadose zone: samples with 2 mg/L to 10 mg/L nitrate-nitrogen had relative $\delta^{15}N$ levels of 5‰ to 12‰, while samples with higher nitrate-nitrogen contained from 0‰ to 6‰ of $\delta^{15}N$. (No $\delta^{15}N$ measurements could be made on samples with less than 2 mg/L nitrate-nitrogen.)

There was significant scatter in these data, corroborating the concept of highly heterogeneous transport. Furthermore, just as there was no significant decrease in nitrate-nitrogen with depth, there was no significant increase in $\delta^{15}N$ with depth, similar to isotopic results at geologically similar Yolo County and Salinas Valley sites (Rolston et al. 1996). Then why was the total nitrogen storage in the deep vadose zone so low?

The nitrate distribution pattern that we found (fig. 7) was similar to that postulated in other experimental studies specifically designed to assess transport in heterogeneous soils as well as that predicted by numerical models of flow and transport in highly heterogeneous vadose zones (Harter and Yeh 1996). Hence, the proposed conceptual framework of preferential flow in the deep vadose zone may provide the answer: preferential flow paths, which are responsible for most of the water and solute transport from the root zone to the water table, quickly flushed nitrate-nitrogen to deeper portions of the vadose zone and to the water table, allowing for little or no denitrification. This would explain the occurrence of high nitrate-nitrogen levels and low $\delta^{15}N$ levels throughout the depth of the vadose zone profile.

Lower nitrate-nitrogen would occur in stagnant water zones outside preferential flow paths. Due to their longer residence time, nitrate-nitrogen in these zones was apparently subject to a small amount of denitrification, which would explain the higher levels of $\delta^{15}N$ that were also found, scattered throughout most of the profile.

The importance of this finding is that while limited denitrification took place in the stagnant water areas of the vadose zone, the majority of the

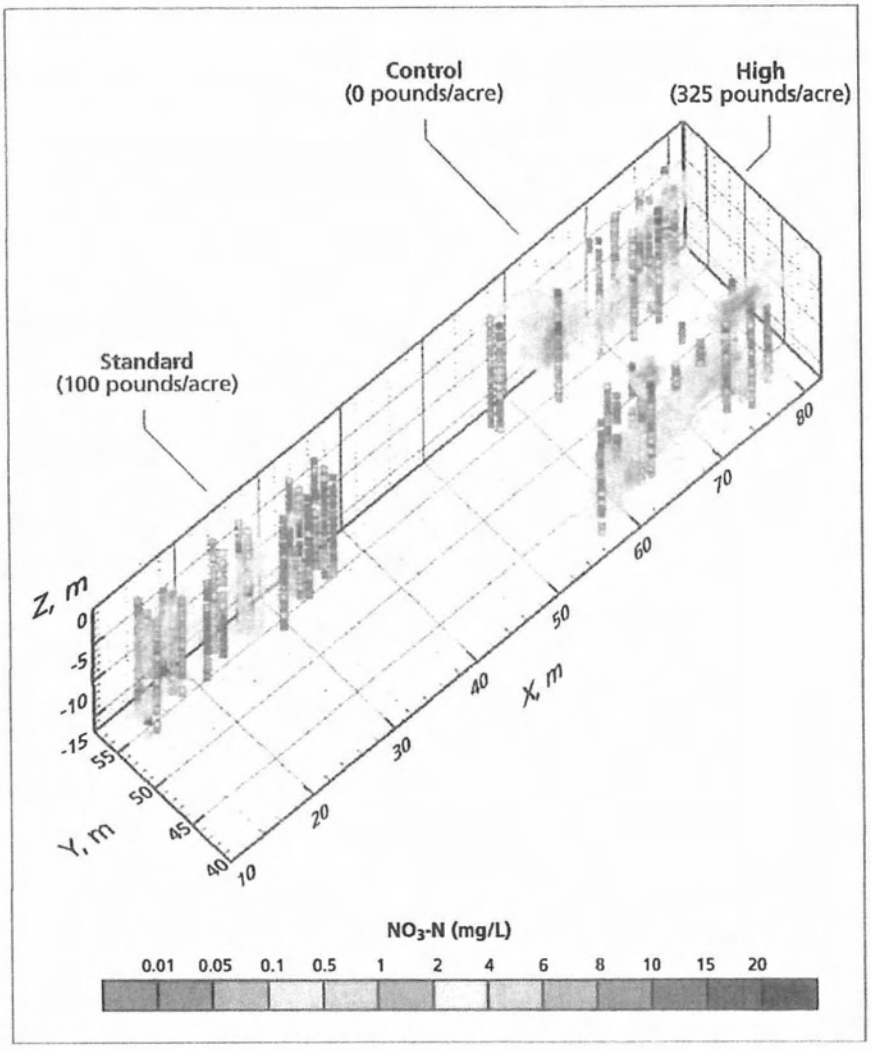

Fig. 7. Measured core nitrate-nitrogen data (squares) and three-dimensional, kriged (yellow) contours of nitrate-nitrogen data. The kriged isosurfaces (only for NO_3-N > 1 mg/L) are obtained from geostatistical analyses of the water content and nitrate measurements at the sampling locations. The standard subplot yielded the largest areas of negligible nitrate concentrations (NO_3-N < 1 mg/L) among the three subplots. High concentrations are seen in the upper profile and near the water table.

nitrate-nitrogen transport occurred in preferential flow paths, where no significant denitrification appears to have taken place. Hence, the low average nitrate-nitrogen concentration in the vadose zone pore water should not be interpreted as an indicator for high denitrification and low nitrate impact on groundwater. Rather, it may be the result of swift, unattenuated nitrate-nitrogen transport to the water table (the same may apply to the root zone).

Analysis shows variability

Our detailed geologic, hydraulic and geochemical analysis of a typical deep vadose zone in the eastern San Joaquin Valley demonstrated that alluvial vadose zones are subject to significant geologic variability, which in turn causes the hydraulic properties and water flow in the vadose zone to exhibit strong spatial variability. While such variability is expressed to only a limited degree in the variability of the observed moisture content, it leads to highly variable concentrations of chemicals, such as nitrate. Our research presents new evidence indicating that unsaturated water flow and transport of nitrate and other agrochemicals (such as pesticides) in the deep vadose zone below the root zone may be subject to significant preferential flow patterns with significantly faster travel times than would be estimated under uniform flow assumptions. Faster travel times not only decrease the potential for denitrification, but also decrease the potential for natural attenuation of pesticides.

Our work suggests that the traditional interpretation of deep vadose zone measurements should be reconsidered. The assumption of uniform flow is not applicable to many alluvial vadose zone sites. The common practice of compositing soil samples taken from immediately below the root zone provides an estimate of the average nitrate-nitrogen concentration at that depth. However, our work indicates that recharge water may constitute only a minor portion of that vadose zone water and is not effectively represented by composite soil samples. It appears that the average or composite nitrate-nitrogen concentrations are also not appropriate for estimating the amount of denitrification as a closure term to the nitrogen mass balance. We are currently implementing detailed heterogeneous flow and transport simulations to further support these findings and to develop guidelines for sampling the deep vadose zone.

T. Harter is Associate Groundwater Quality Hydrologist (UC Cooperative Extension), Department of Land, Air and Water Resources, UC Davis; Y.S. Onsoy is consultant and Doctoral Candidate, UC Davis; K. Heeren is freelance geologist in environmental education, Germany; M. Denton is

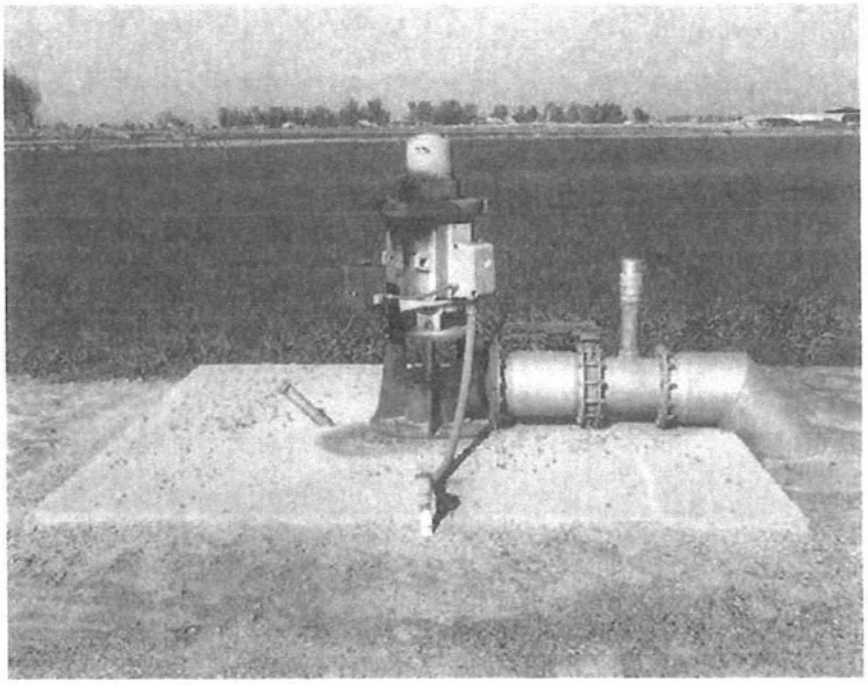

Before it is pumped to the surface for agricultural or other uses, groundwater percolates through the geologically variable vadose zone. Based on this study, current assumptions about transport of nitrate from fertilizers and other agricultural chemicals need to be reexamined.

consultant and obtained a master's degree in hydrologic studies, Department of Land, Air and Water Resources, UC Davis; G. Weissmann is Assistant Professor of Hydrogeology, Department of Geological Sciences, Michigan State University; and J.W. Hopmans is Professor of Vadose Zone Hydrology, and W.R. Horwath is Associate Professor of Soil Biogeochemistry, Department of Land, Air and Water Resources, UC Davis.

The California Fertilizer Research and Education Program, California Tree Fruit Agreement, UC Water Resources Center, Geoprobe Systems and Studienstiftung des Deutschen Volkes provided support for this project. We would like to thank Kevin Pope, formerly with Geoprobe Systems, Jean Chevalier with his crew at KREC, and Dick Rice and R. Scott Johnson at the UC Kearney Agricultural Center for their support during the field work; Anthony Cole, Chad Pyatt and Rigo Rios for drilling the 3,000 feet of vadose zone cores at the site; Andrea DeLisle and Timothy Doane for their analytical chemistry work; Jim MacIntyre for implementation of the multistep outflow experiments needed to determine the hydraulic properties at the site; and Atac Tuli for his support in developing the necessary software to use in conjunction with the multistep outflow experiments.

References

Gilliam JW, Dasberg S, Lund LJ, Focht DD. 1978. Denitrification in four California soils: Effect of soil profile characteristics. Soil Sci Soc Amer 42:61–6.

Glass RJ, Yarrington L. 2003. Mechanistic modeling of fingering, nonmonotonicity, fragmentation, and pulsation within gravity/buoyant destabilized two-phase/unsaturated flow. Water Resour Res 39(3):1058, DOI:10.1029/2002WR001542.

Harter T, Yeh T-CJ. 1996. Stochastic analysis of solute transport in heterogeneous, variably saturated soils. Water Resour Res 32(6):1585–95.

Huntington GL. 1980. Soil-land form relationships of portions of the San Joaquin River and Kings River alluvial depositional systems in the Great Valley of California. Ph.D. dissertation, UC Davis. 147 p.

Johnson RS, Mitchell FG, Crisosto CH. 1995. Nitrogen fertilization of Fantasia nectarine: A 12-year study. UC Kearney Tree Fruit Rev 1:14–9.

Klein JM, Bradford WL. 1979. Distribution of nitrate and related nitrogen species in the unsaturated zone, Redlands and vicinity, San Bernardino County, California. USGS Water Resourc Invest Rep 79–60. 81 p.

Kung K-JS. 1990. Preferential flow in a sandy vadose zone: 1. Field observations. Geoderma 46:51–8.

Lund LJ, Adriano DC, Pratt PF. 1974. Nitrate concentrations in deep soil cores as related to soil profile characteristics. Environ Qual 3:78–82.

Marchand DE, Allwardt A. 1981. Late Cenozoic stratigraphic units, northeastern San Joaquin Valley, California. USGS Bull 1470.

Minasny B, Hopmans JW, Harter T, et al. 2003. Neural networks prediction of soil hydraulic functions from multi-step outflow data. Soil Sci Soc Amer 68:417–29.

Onsoy YS, Harter T, Ginn T, Horwath WR. 2005. Spatial variability and transport of nitrate in a deep alluvial unsaturated zone. Vadose Zone J 4(1):41–54.

Page RW, LeBlanc RA. 1969. Geology, hydrology and water quality in the Fresno area, California. USGS Open-File Rep. 70 p.

Pratt PF, Jones WW, Hunsaker VE. 1972. Nitrate in deep soil profiles in relation to fertilizer rates and leaching volume. Environ Qual 1:97–102.

Rees TF, Bright DJ, Fay RG, et al. 1995. Geohydrology, water quality, and nitrogen geochemistry in the saturated and unsaturated zones beneath various land uses, Riverside and San Bernardino Counties, California, 1991–93. USGS Water Resour Invest Rep 94–4127. 267 p.

Retallack GJ. 1990. *Soils of the Past — An Introduction to Paleopedology*. Hyman U (ed.). Winchester, MA. 520 p.

Rolston D, Fogg GE, Decker DL, et al. 1996. Nitrogen isotope ratios identify nitrate contamination sources. Cal Ag 50(2):32–6.

Russo D, Zaidel J, Laufer A. 1998. Numerical analysis of flow and transport in a three-dimensional partially saturated heterogeneous soil. Water Resour Res 34(6):1451–6.

Wang Z, Wu L, Harter T, et al. 2003. A field study of unstable preferential flow during soil water redistribution. Water Resour Res 39(4), 10.1029/2001WR000903, 01 April 2003.

Weissmann GS, Mount JF, Fogg GE. 2002. Glacially-driven cycles in accumulation space and sequence stratigraphy of a stream-dominated alluvial fan, San Joaquin Valley, California. J Sediment Res 72:270–81.

Flury, M. 1996. Experimental evidence of transport of pesticides through field soils—A review. J. Environ. Qual. 25:25–45.
Ghodrati, M., and W.A. Jury. 1992. A field study of the effects of soil structure and irrigation method on preferential flow of pesticides in unsaturated soil. J. Contam. Hydrol. 11:101–125.
Gish, T.J., C.S. Helling, and B. Wienhold. 1990. Time dependent adsorption of five herbicides in field soil. p. 211. 1990 Agron. Abstracts. ASA, Madison.
Gusfafson, D.I. 1989. Groundwater ubiquity score: A method for assessing pesticide leachability. Environ. Toxicol. Chem. 8:339–357.
Helling, C.S., and T.J. Gish. 1991. Physical and chemical processes affecting preferential flow. p. 77–86. *In* T.J. Gish and A. Shirmohammadi (ed.) Preferential flow. Proc. Natl. Symp., Chicago. 16–17 Dec. 1991. ASAE, St. Joseph, MI.
Ju, S.-H., K.-J.S. Kung, and C. Helling. 1997. Simulating impact of funnel flow on contaminant sampling in sandy soils. Soil Sci. Soc. Am. J. 61:409–415.
Kladivko, E.J., G.E. Van Scoyoc, E.J. Monke, K.M. Oates, and W. Pask. 1991. Pesticide and nutrient movement into subsurface tile drains on a silt loam soil in Indiana. J. Environ. Qual. 20:264–270.
Kladivko, E.J., L.C. Brown, and J.L. Baker. 1999. Pesticide transport to subsurface tile drains in humid regions of North America. Rep. to the Am. Crop Protection Assoc. W. Lafayette, IN.
Kung, K-J.S. 1990. Preferential flow in a sandy vadose zone: 1. Field observation & 2. Mechanism and implications. Geoderma. 46: 51–71.
Kung, K.-J.S., E. Kladivko, T. Gish, T.S. Steenhuis, G. Bubenzer, and C.S. Helling. 2000. Quantifying preferential flow by breakthrough of sequentially-applied tracers: Silt loam soil. Soil Sci. Soc. Am. J. 64:1296–1304 (this issue).
Luxmoore, R.J. 1991. On preferential flow and its measurement. p. 113–121. *In* T.J. Gish and A. Shirmohammadi (ed.) Preferential flow. Proc. Natl. Symp. Chicago. 16–17 Dec. 1991. ASAE, St. Joseph, MI.
Richards, T.L., and T.S. Steenhuis. 1988. Tile drain sampling of preferential flow on a field scale. *In* P.F. Germann (ed.) Rapid and far reaching hydrological processes in the vadose zone. J. Contam. Hydrol. 3:307–325.
Roth, K., W.A. Jury, H. Fluhler, and W. Attinger. 1991. Transport of chloride through an unsaturated field soil. Water Resour. Res. 27:2533–2541.

Quantifying Preferential Flow by Breakthrough of Sequentially Applied Tracers: Silt Loam Soil

K.-J. S. Kung,* E. J. Kladivko, T. J. Gish, T. S. Steenhuis, G. Bubenzer, and C. S. Helling

ABSTRACT

Field experiments were conducted on tile-drained plots at the South East Purdue Agricultural Center in Butlerville, Indiana, to quantify contaminant transport via preferential flow paths in a silt loam soil. Breakthrough patterns of three fluorobenzoic acids (pentafluorobenzoic acid [PFBA], *o*-trifluoromethylbenzoic acid [*o*-TFMBA], and 2,6-difluorobenzoic acid [2,6-DFBA]) in a preliminary study indicated that they were transported as conservatively as is bromide (Br^-). These four tracers were then sequentially applied, in an adjacent plot, during simulated precipitation (3 mm h^{-1} intensity, 10-h duration). Bromide was sprayed shortly before irrigation started, while PFBA, *o*-TFMBA, and 2,6-DFBA were applied at 2, 4, and 6 h thereafter, respectively. Tile flow began increasing at around 3 h, and Br^- appeared in tile drain flow ≈4 h after irrigation started, yet benzoic acids, PFBA, *o*-TFMBA, and 2,6-DFBA, were detected in the tile drainage at 102 min, 42 min, and 18 min after their applications, respectively. Tracer mass recovery from tile drainage was Br^- (7.04%), PFBA (13.9%), *o*-TFMBA, (18.7%), and 2,6-DFBA (19.7%) of applied mass. The faster arrival time and greater recovery of sequentially applied tracers confirmed that water movement and contaminant transport shifts toward increasingly larger pores of the preferential flow paths as soil becomes wet during a precipitation event. The breakthrough patterns of these tracers can be used to quantify the water flux distributions of preferential paths. Because ≈90% of the chemical leached from this precipitation event occurred during the first day, it was critical to intensively monitor contaminant transport during the first 24 h after a rainfall. A soil sampling protocol based on collecting soil cores at random locations once every several days is unsuitable for determining the deep leaching under field conditions.

K.-J.S. Kung, Dep. of Soil Science; and G. Bubenzer, Dep. of Biol. System Eng., Univ. of Wisconsin, Madison, WI 53706-1299; E.J. Kladivko, Dep. of Agronomy, Purdue Univ., West Lafayette, IN; T.S. Steenhuis, Dep. of Agric. and Biol. Eng., Cornell Univ., Ithaca, NY 14850; T.J. Gish, Hydrology Lab., and C.S. Helling, Weed Science Lab., USDA-ARS, BARC-W, 10300 Baltimore Blvd., Beltsville, MD 20705-2350. Received 2 Feb. 1999. *Corresponding author (kung@calshp.cals.wisc.edu).

Published in Soil Sci. Soc. Am. J. 64:1296–1304 (2000).

FERTILIZERS AND PESTICIDES have played essential roles in helping to provide high agricultural output per unit area of arable land. After extensive use, however, some chemicals have resulted in non-point water contamination. Water contamination by pesticides and nitrate is now perceived as one of our nation's most significant, long-term environmental problems. During the last three decades, researchers have sought to understand the fundamental transport processes leading to water contamination, hoping thereby to eventually diminish its impact. Soil physicists have focused tremendous effort on measuring soil hydraulic properties and devising statistical methods to comprehend their spatial variability; this is based on the premise that one must first quantify water flux distribution before solute transport can be resolved. On the other hand, soil chemists and microbiologists have characterized adsorption and degradation of agrichemicals, in part assuming that the leaching of agrichemicals can be minimized if optimum combinations of adsorption and degradation can be achieved.

Currently, efforts to directly measure soil hydraulic properties have been gradually decreasing because field results show that, with limited budget and instruments, the soil hydraulic properties and their spatial and temporal variability are too complex to be grasped, and field-scale water flux distribution cannot be directly and adequately characterized. Furthermore, results from field experiments demonstrated that strongly adsorbing chemicals can move as fast and deep into a soil profile as more mobile chemicals. For example, using a tile drain as an alternative sampling protocol, Everts et al.

Abbreviations: BTC, breakthrough curve; HPLC, high performance liquid chromatography; IC, ion chromatography; *o*-TFMBA, *o*-trifluoromethylbenzoic acid; PFBA, pentafluorobenzoic acid; WT, water tracer; 2,6-DFBA, 2,6-difluorobenzoic acid.

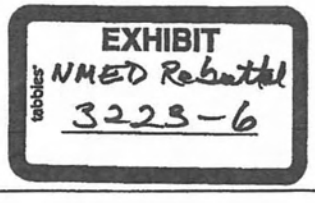

(1989) observed that both non-adsorbing Br^- and adsorbing rhodamine water tracer (WT) dye had fast breakthrough patterns within the first 4 h after the initiation of the irrigation. Kladivko et al. (1991, 1999) demonstrated that pesticides were most susceptible to leaching during rainstorms that occur shortly after chemical application in spring, and more adsorbing pesticides atrazine [2-chloro-4-(ethylamino)-6-(isopropylamino)-*s*-triazine] and alachlor [2-chloro-2′,6′-diethyl-*N*-(methoxymethyl)-acetanilide] can be transported to shallow groundwater (between 0.8–1.0 m) as rapidly as more mobile chemicals such as carbofuran (2,3-dihydro-2,2-dimethyl-7-benzofuranol methylcarbamate) during this period. Kung et al. (2000) applied a pulse of chloride and rhodamine WT dye solution in a field experiment on a clay loam soil. They found that both tracers arrived at the tile after 13 min after application. Saturated soil hydraulic conductivity of the field, based on soil cores collected at different depths, ranged from 0.5 to 5.0 $\times$ 10^{-6} m s^{-1}. According to the conventional conceptualization, neither the conservative nor the reactive tracers should have reached the tile drain within 2 d.

The term *preferential flow paths* was coined to describe the fast contaminant transport that bypassed the vast soil matrix (Kung, 1990). It is critical to comprehend preferential flow in order to develop conceptual and numerical models to predict contaminant transport in unsaturated soils. Ju and Kung (1997) conducted numerical experiments in sandy soils with layering structures to characterize the water dynamics of the funnel-type preferential flow pathways and their impact on contaminant transport in an unsaturated sandy soil profile. They justified their numerical approach by the following two reasons: (i) the impact of a funnel mechanism that is caused by layered structure on contaminant transport was well understood (Kung, 1993; Ju and Kung, 1993); and (ii) the multiple-layered soil structures in an unsaturated sandy profile that trigger funnel flow are permanent and can be characterized by the ground-penetrating radar technique (Kung and Lu, 1993; Casper and Kung, 1996). In contrast, in unsaturated soils with finer textures, field-scale preferential flow mechanisms are not expressly understood. The preferential flow paths have a dynamic formation–destruction cycle, and there are no instruments to accurately map or reveal these paths. The preferential flow paths are three-dimensional, occupy only a very small volumetric fraction of the soil matrix, and cannot be quantified by the conventional techniques designed to measure the hydraulic properties of the bulk soil matrix. Therefore, the impacts of preferential flow paths on contaminant transport in fine-textured soils still cannot be numerically examined.

Jury (1982) introduced the *transfer function* concept to bypass the necessity of accurately and directly measuring the soil hydraulic properties of unsaturated soils in order to predict contaminant transport. In his approach, the breakthrough curve (BTC) of a conservative tracer was used to reflect the convoluted impact of the water dynamics on solute transport under field conditions. Jury's concept was adopted in this study; i.e., BTCs of conservative tracers were used to quantify the impact of the water dynamics of preferential flow on solute transport. In Jury's approach, the breakthrough of a single pulse of a conservative tracer was used and it was implicitly assumed that the water flux distribution was a stationary property of a soil profile. The rainfall intensity–duration from individual precipitation events were not considered as parameters. Instead, only the total net infiltration from all precipitation events during a period was used to drive the contaminant transport.

Experimental results from Kung et al. (2000) showed that as a soil profile became wetter during a precipitation event, the arrival time of both conservative and reactive tracers to a tile drain shortened. This indicated that the water flux distribution of preferential flow paths change during a precipitation event; i.e., some preferential flow paths were not hydraulically active when a soil profile was initially dry. This implied that the water flux distribution of preferential flow paths was not a stationary property of a soil profile but depended primarily on soil water content of the soil profile. As a result, each rainfall event can have a different impact on the contaminant transport through preferential paths. In this study, different conservative tracers were sequentially applied during a single precipitation event. As the soil surface became wetter, the breakthrough patterns of tracers applied at different times reflected the impact of the change of the pore spectrum of hydraulically active preferential flow paths on contaminant transport.

The success of using a chemical BTC to quantify the water dynamics of preferential flow paths hinged on whether a representative breakthrough pattern could be measured to accurately reflect the convoluted impact of water fluxes along preferential flow paths on contaminant transport. As demonstrated by Ghodrati and Jury (1990), Ju et al. (1997), and Kung et al. (2000), conventional sampling protocols (e.g., soil coring and soil lysimeter methods) are unsuitable to monitor the field-scale chemical leaching patterns through preferential flow paths. Richards and Steenhuis (1988), Kladivko et al. (1991, 1999), and Czapar et al. (1994) showed that tile drain facilities can be used as an alternative.

Multiple conservative tracers with similar properties must first be chosen in order to reflect the impact of preferential flow paths on contaminant transport as a soil profile becomes wetter. Currently, Br^- and Cl^- are regarded as the most suitable conservative tracers and are commonly used to indicate water movement and solute transport. Bowman and Gibbens (1992) and Jaynes (1994) explored the transport properties of several fluorobenzoic acids, comparing them with Br^-. Among the tested fluorobenzoic acid isomers, three were recommended (because they had the least adsorption and degradation) as alternative conservative tracers: PFBA, 2,6-DFBA, and *o*-TFMBA. The breakthrough patterns of these alternative tracers were rigorously tested in laboratory soil column studies (Jaynes, 1994). Under field conditions, only their recoveries in soil matrix from soil cores were compared, and the deep leaching through preferential paths could not be assessed by the soil coring method.

In this study, the primary objective was to use a tile

drain monitoring facility to quantify the water dynamics of the preferential flow pathways and their impact on contaminant transport in a fine-textured, unsaturated soil profile. A preliminary experiment was first conducted to determine whether the three fluorobenzoic acids mentioned above would have the same breakthrough patterns as those of Br^- and Cl^- under field conditions in a soil profile with preferential flow paths. Although not a conservative tracer, nitrate has recently been blamed as a major cause of oxygen-depleted water (hypoxic zone) in the Gulf of Mexico and the USA. U.S. Geological Survey data indicated that >70% of the total N delivered to the Gulf by the Mississippi River originates above the confluence of the Ohio and Mississippi Rivers (Alexander et al., 1995; USDA-NRCS, 1996). A secondary objective of the preliminary study was to determine whether Br^-, Cl^-, and these fluorobenzoic acids have the same breakthrough patterns as freshly applied nitrate in a soil profile with preferential flow paths. After examining the suitability of three alternative tracers, the objective of our main experiment was then to quantify the water dynamics of preferential flow paths and their impact on contaminant transport in an unsaturated silt loam soil.

MATERIALS AND METHODS

Preliminary Study

Experiments were conducted in a field at the South East Purdue Agricultural Center of Purdue University in Butlerville, Indiana, in November 1996. This site was chosen because tile monitoring stations had been installed in the early 1980s and preferential flow had been observed (Kladivko et al. 1991, 1999). The cropping system was a corn–soybean rotation and the soil had been under no-till management for three years. The slope at the site is approximately 1%. The experimental plot is 225 m long and 20 m wide, with a center tile drain that is monitored for flow and chemical flux. Border tiles (not monitored) at 10 m on either side of the center tile were installed to accurately partition the water input area to the center tile. The soil is Clermont silt loam soil (fine-silty, mixed, superactive, mesic Typic Glossaqualfs) with approximately 20% sand, 70% silt, and 10% clay. This loess soil has ≈1% soil organic matter in the top 45-cm depth and is typical of the southern portion of very extensive Midwest Corn Belt soils, extending from southwestern Ohio, across southern Indiana and southern Illinois, through Missouri, into southern Iowa and eastern Kansas (Kladivko et al., 1991). The perched groundwater at this site is maintained at approximately 0.75- to 0.9-m depth by tile drainage.

The five conservative tracers Br^-, Cl^-, PFBA, 2,6-DFBA, *o*-TFMBA, as well as nitrate, were co-applied to determine whether they had similar breakthrough patterns. The total masses of tracers applied were Br^- (2.0 kg), Cl^- and nitrate (2.4 kg each), and the benzoic acids (0.45 kg each). Each chemical was first dissolved separately (pH of each benzoic acid solution was adjusted to 7 by slowly adding KOH solution), and then all were combined into a ≈115-L tank mix to be applied uniformly through a sprayer. In most published results from field experiments, chemicals were applied to an entire field. However, in this preliminary study, the six tracers were applied only to a 1.5-m by 24-m strip. The long side of the strip was parallel to the long side of the plot and offset 0.3 m from the center tile line. The down-slope end of the chemical strip was located 33 m from the lower end of the field. The main reason for applying chemicals only to a strip was to reduce cost, because the benzoic acids were too expensive to be used throughout the entire field. This preliminary study was only to determine whether the benzoic acids had similar BTCs to those of Br^-, Cl^-, and nitrate. Also, because the watertable near the tile line has the steepest gradient, applying chemicals to a narrow strip close to the tile line could minimize the time required for the lateral transport of chemicals within a saturated zone to the tile line, so that the travel time of contaminants through preferential flow paths within the unsaturated soil profile can be accurately estimated.

In order to bring the watertable up to the tile line, the site had been pre-irrigated with ≈15 mm water (6.2 mm h^{-1} intensity) one day before the experiment with a solid-set sprinkler system. Then on the morning of the experiment, a 1-h pre-irrigation added another 6.2 mm water. After waiting for an hour, tracers were applied. Shortly after the tracer application, irrigation with the same intensity was applied for 35 min to leach these chemicals into the soil profile. The chemical application strip was located in the center of the irrigated area (24 m × 60 m). Again, the long sides of the irrigated area and the plot were parallel. Because of the plot's configuration (border tiles 10 m offset from the center tile), a 24-m-wide irrigation width extended beyond the adjacent border tiles and ensured that leachate originated from the treated chemical strip would only enter the center tile being monitored. The irrigation water was from the local municipal water supply and had none of the applied chemicals, except for 2.5 mg L^{-1} Cl^-.

After the chemical application and initial irrigation, there were a 15-mm rainfall (Day 1), a 6.2-mm irrigation (Day 3), 11.7-mm of precipitation (Day 5), and 5.8-mm of precipitation (Day 8). The tile flow was continuously measured by the tipping-bucket method. Water samples were collected from the tile flow to determine the mass flux of these chemicals. The frequency of water sample collection was determined by the flow rate of the tile drainage. For example, shortly after each irrigation or precipitation event, when tile flow was relatively high, a 100-mL sample was collected every 10 min and three such samples were composited into a final water sample. As tile flow started to decrease, 100-mL samples were collected at 20-min intervals and three samples were composited into a final water sample. About two days after each irrigation or precipitation event, a 50-mL sample was collected at 30-min intervals and six samples were composited.

Main Experiments of Sequentially Applied Conservative Tracers

Field experiments were conducted at another 20-m by 225-m no-till plot at the South East Purdue Agricultural Center in Butlerville, Indiana, in May of 1997, when corn was starting to emerge. The tile flow rate was ≈1 mL s^{-1} (caused by a 1.2-cm pre-irrigation event 2 d earlier) and there was no precipitation in the five-day weather forecast. Irrigation (3 mm h^{-1} intensity) was continuously applied for 10 h to simulate a prolonged mild spring shower by a solid-set sprinkler system. The sprinkler system was made of two lines that were 12 m apart. Within each line, the distance between two adjacent nozzles was 12 m. Nozzles between the two lines were staggered by 6 m. The low intensity was chosen to avoid any surface runoff so that mass recovery could be accurately calculated. The irrigated area (24 m × 60 m) was about 73 m from the lower end of the field, where the tile monitoring facility was installed.

The conservative tracers tested in the preliminary study

were sequentially applied. Shortly before the irrigation started, Br^- (1.93 kg in 20 L water) was uniformly sprayed on a 1.5-m by 24-m strip. The strip was positioned at the center of the irrigated area and the long side of the strip was parallel to the tile line with 0.3 m offset. At 2 h after irrigation commenced, PFBA (1.37 kg in 16 L water) was sprayed on the same strip. Then, at 4 and 6 h after the irrigation started, *o*-TFMBA (1.5 kg in 16 L water) and 2,6-DFBA (1.5 kg in 20 L water) were sprayed on the same strip, respectively. For each acid tracer solution, pH was adjusted to 7 by slowly adding KOH solution during mixing. Each tracer was applied through a sprayer within ≈5 min; irrigation was continuous when tracers were applied. This sequential tracer application scheme was intended to explore how water and tracers would move through the larger end of the pore spectrum of preferential flow paths as a soil profile became wetter.

During the first 12 h after the irrigation started, water samples were collected from the tile once every 6 min. From 12 h to 24 h, water samples were collected at 10-min intervals and sequentially composited into 30-min samples. From the second to the fourth days, samples were collected every 40 min, with three samples composited to give 2-h samples. This intense sampling frequency was designed to register the fast contaminant breakthrough observed by Kung et al. (2000). The samples were stored at 5°C until analyzed, except during a short period of shipping. Flow rate of the tile drain was continuously measured by using the tipping-bucket method.

Chemical Analyses

A 3-mL aliquot from each sample was filtered (0.2 μm) and then analyzed by high performance liquid chromatography (HPLC) for the benzoic acids and by ion chromatography (IC) for Br^-, Cl^-, and nitrate. The HPLC conditions were as follows: mobile-phase, acetonnitrile 15 m*M* KH_2PO_4 (titrated to pH 2.6 with phosphoric acid) (35:65, v/v); flow rate, 1.7 mL min^{-1}; guard column, Spherisorb SAX (10 mm × 4.6 mm × 5-μm i.d.; Waters, Milford, MA); analytical column, Supelcosil SAX1 (25 cm × 4.6 mm × 5-μm i.d.; Sigma-Aldrich, St. Louis); injection volume, 50 μL; and UV detection, 205 nm. The detection limit for each benzoic acid was 50 μg L^{-1}. The IC conditions were: mobile-phase, 1 m*M* $C_8H_5KO_4$ (titrated to pH 2.6 with NaOH); guard column, Waters IC-Pak anion; analytical column, IC-Pak anion (5 cm × 4.6 mm × 5-μm i.d.); and injection volume, 50 μL. The detection limit for of Br^-, Cl^-, and nitrate were 0.25, 0.5, 0.5 mg L^{-1}, respectively.

RESULTS AND DISCUSSION

Preliminary Study

The mass flux normalized by the mass applied of each tracer sampled from the tile drain during the first 10 days after chemical application is shown in Fig. 1. The results indicated that all tracers had very similar breakthrough patterns. The similarity of these leaching patterns confirmed that the three benzoic acids were as conservative as Br^-, Cl^-, and nitrate. This suggested that it was valid to use these three benzoic acids to quantify water movement in a soil profile with preferential flow paths. The similarity between the mass flux pattern of nitrate and those of the other five tracers indicated that it was also valid to use the breakthrough of conservative tracers to indicate the transport of recently surface-applied nitrate through preferential flow paths. However, it must be stressed that this similarity was partly because this field experiment was conducted in November 1996, when the temperature of the soil profile measured in a nearby weather station fluctuated between 3 to 15°C. There was little microbial activity for N transformation and no nitrate uptake by plant roots during this period.

The BTCs of Cl^- and nitrate in Fig. 1 are higher than the rest because some Cl^- and nitrate were already stored in the soil profile before the tracer application from this experiment. The concentrations of Cl^- and nitrate in the background flow from the tile drain before the chemical application of this experiment were 8.4 and 4.5 mg L^{-1}, respectively, while the concentrations of the other tracers were below their detection limits. That Cl^- had higher mass recovery was partly because there was 2.5 mg L^{-1} Cl^- in the irrigation water. The total mass recoveries during the first 10 days were Br^- (2.59%), 2,6-DFBA (2.41%), *o*-TFMBA (2.56%), and PFBA (2.50%). The mass recoveries of Cl^- and nitrate were unknown because it was impossible to partition the percentages of these two chemicals contributed from the soil matrix.

Main Experiment: Sequentially Applied Tracers

Based on 55 rain gauges, the measured total water applied during the 10-h irrigation was 28.8 mm with the Christianson uniformity of 0.85. The measured breakthrough patterns of the four applied tracers and the tile hydrograph are shown in Fig. 2. The tile hydrograph showed that tile flow started to increase at 2 h and 50 min after irrigation started. Bromide was applied shortly before the irrigation started, while the PFBA was applied 2 h after the irrigation started. According to the conventional conceptualization of Darcian flow and convection–dispersion transport, Br^- should reach the shallow groundwater first (i.e., first in, first out); however, PFBA was detected in the tile drainage at 3 h and 42 min after the irrigation started (i.e., 102 min after its application), while Br^- was not detected until 4 h after its application. On the other hand, the *o*-TFMBA was applied at 4 h after the irrigation and arrived at the tile 4 h 42 min after the irrigation started (i.e., only 42 min after its application). The fourth tracer, 2,6-DFBA, was applied at 6 h after the irrigation began and arrived at the tile at only 18 min after its application. Figure 2 shows that the mass flux of the 2,6-DFBA at the first detection is much higher than those of the other three tracers. The water samples were collected once every 6 min in the first 12 h. It was very possible that the 2,6-DFBA actually first appeared in the tile drain shortly after the water sample taken at 12 min after application.

Water movement and contaminant transport occurs through a spectrum of pores in an unsaturated soil under field conditions. The preliminary study had already shown that the four tracers were equally mobile through the preferential flow paths, while the main study showed that the later a tracer was applied during a simulated precipitation event, the faster the tracer arrived at the tile line. The dramatically shorter transit time for a

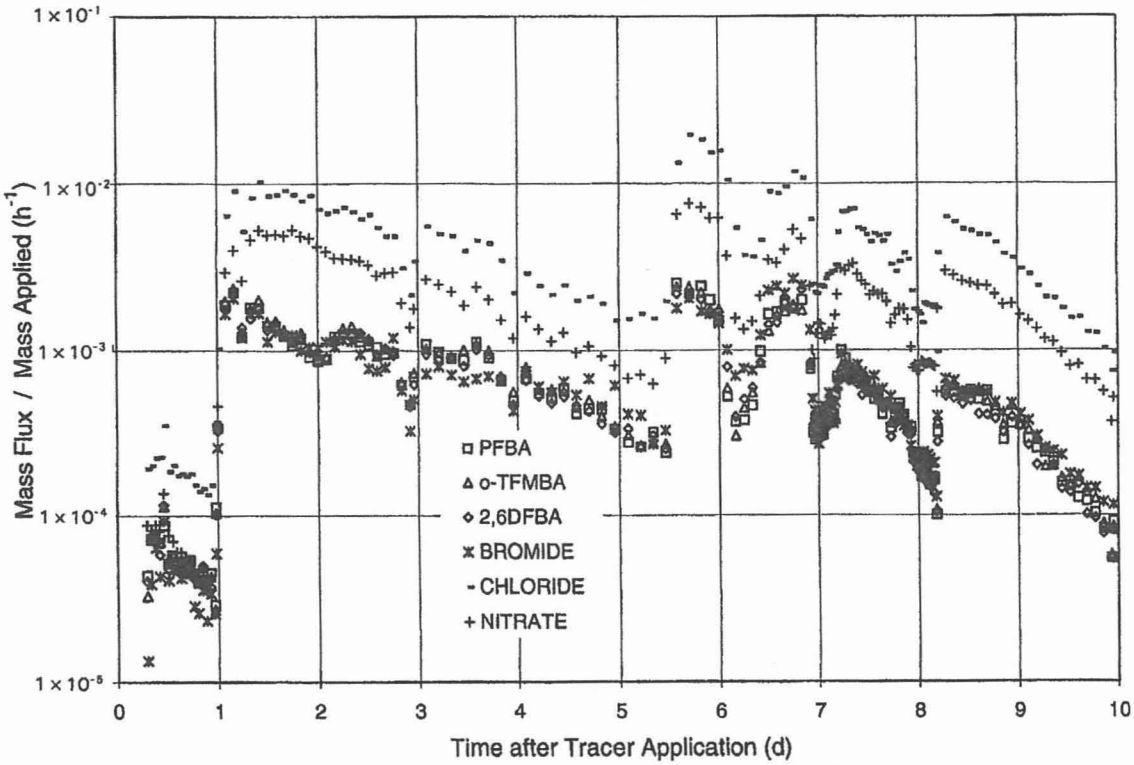

Fig. 1. The mass flux of six chemicals during the first 10 days, while each was normalized by its applied mass.

tracer applied at later time indicated that different preferential flow paths were utilized for different tracers; i.e., the fourth tracer was transported through preferential flow paths with the largest pores, hence, arriving fastest at the groundwater surface. The slower breakthrough for the tracers applied earlier was because water and water-borne chemicals were sucked into the matrix pores along wall of the pathways when the profile was dry.

A preferential flow path is defined as hydraulically active when water and water-borne contaminants can directly reach the shallow groundwater surface through the preferential flow pathway. Let us assume there is a preferential flow path labeled "A". The tracers applied earlier entered into the Pathway A and were later sucked into small matrix pores along wall of the Pathway A. On the other hand, let us assume that the tracers applied later entered into the identical preferential flow Pathway A and reached groundwater through the Pathway A. Although both tracers passed through certain identical portions of flow Pathway A, the tracers should be considered to have traveled through two different flow paths. Because Br^- from the first tracer pulse could not directly reach the shallow groundwater surface through the Pathway A, the preferential flow Pathway A was not hydraulically active to transport Br^-. Alternatively, it can be said that Br^- had traveled through a preferential flow Pathway B, which was made of two parts. The first part was made of the upper part of preferential flow Pathway A, while the lower part was made of some matrix pores. Therefore, the Pathway B had a smaller overall equivalent pore size than that of Pathway A. Later, when the soil profile became wet enough, the preferential flow Pathway A became completely hydraulically active to the fourth tracer. In other words, it can be described that preferential flow paths with larger equivalent pore sizes became hydraulically active later, when a soil profile became wetter.

The mechanism in which applied water and tracers would enter pores of a wide size-spectrum was not considered as a parameter in the conventional conceptualization of Darcian flow and convective–dispersive transport. As a result, a tracer applied early was expected to arrive at the tile first. The fact that Br^- had the slowest arrival time indicated that the larger end of the pore spectrum of the preferential flow paths were not hydraulically active when the soil surface was relatively dry. Therefore, it is critical to consider how and when contaminants enter preferential flow paths with different pore sizes. The overall results from four tracers indicated that, as a soil profile becomes wetter during precipitation, water movement and contaminant transport would continuously shift toward the larger end of the pore spectrum of the preferential flow paths.

The tracer recovery (percentage of total applied mass) from tile drainage during the 100-h period were Br^- (7.04%), PFBA (13.9%), o-TFMBA, (18.7%), and 2,6-DFBA (19.7%). The mass leached increased among the sequentially applied tracers; i.e., the later a tracer was applied, the more mass was leached. The fact that Br^- had the least mass leached and the 2,6-DFBA had the most was consistent with their arrival times; i.e., Br^- arrived the latest and the 2,6-DFBA arrived the earliest after application. Because Br^- was applied to a rela-

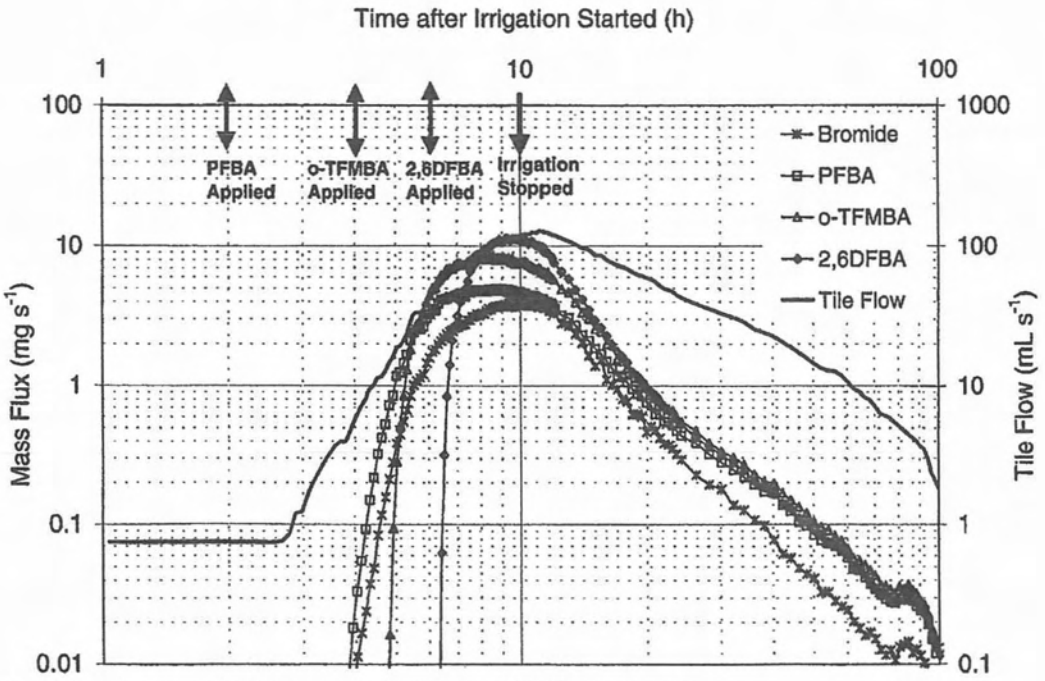

Fig. 2. The breakthrough curves of the four conservative tracers and tile flow hydrograph.

tively dry soil surface before the irrigation started, it had the least chance of being transported through the preferential flow paths. As a result, most of the applied Br^- entered into the smaller end of the pore spectrum, was transported more slowly, and still remained in the soil matrix after 100 h. The mass recovery patterns confirmed that, when a soil profile became wetter during a prolonged precipitation event, contaminant transport would be continuously shifted toward the larger end of the pore spectrum of the preferential flow paths. The primary reason that mass recovery of Br^- from this study was higher than that observed in the preliminary study was because the rain duration was much shorter in the preliminary study. In a precipitation event with very short duration, matric potential gradient would induce a tracer to enter into and be transported through the soil matrix pores.

These high recoveries after such a mild irrigation with only 28.8 mm total water applied were surprising. Note that in the preliminary experiment where ≈39 mm water was applied in a 10-d period, only ≈2.5% of the applied mass of each tracer was leached out. This was because the rain duration was short during the preliminary experiment. As a result, the tracers applied in the preliminary experiment had a better chance to enter the smaller matrix pores and became less susceptible to deep leaching through preferential flow paths.

Figure 2 shows that vast majority of the tracer recovered from the tile drain during the 100-h sampling period leached out from the root zone during the first day after the irrigation started (i.e., Br^-, 90%; PFBA, 87%; *o*-TFMBA, 89%; and 2,6-DFBA, 91%), which is also when most of the water flow occurred. According to the comparison between the BTC of adsorbing and non-adsorbing tracers, Kung et al. (2000) found that the tail of the adsorbing tracer BTC trailed much faster than those of the non-adsorbing tracers. In other words, an adsorbing chemical had more of its leaching occur during the first day than a non-adsorbing chemical.

Among the deterministic models which simulate fast solute leaching through soil structural pores, the two-region (or two-domain) *mobile–immobile* conceptualization (Skopp and Warrick, 1974) was first proposed to explain the fast leaching observed in aggregated soils under laboratory conditions. Gerke and van Genuchten (1993) proposed the *dual porosity* model, in which water and solutes moved through two distinct and interacting domains simultaneously. Similarly, Gwo et al. (1995) proposed a multiple-porosity model, where soil is partitioned into many interacting domains. The arrival times and mass recovery patterns from our sequentially applied tracers and those from Kung et al. (2000) showed that the spectrum of hydraulically active preferential flow paths expanded continuously during a precipitation event; i.e., preferential flow paths with larger pore sizes became hydraulically active and contributed to contaminant transport as a soil profile became wetter. Because 90% or more of the contaminants that leached from the root zone in the 100-h sampling period were leached during the first 24 h through preferential flow paths, the contribution of the so-called *immobile*, or *matrix flow*, or *micropore* domain to contaminant transport was almost irrelevant during this time frame. Whether those contaminants that entered into soil matrix pores could move back into preferential flow paths and reach the watertable during subsequent precipitation events was beyond the scope of the current study.

One can use the BTCs of the sequentially applied tracers to make inferences about the behavior of freshly applied nitrate fertilizers, since the short time scale of

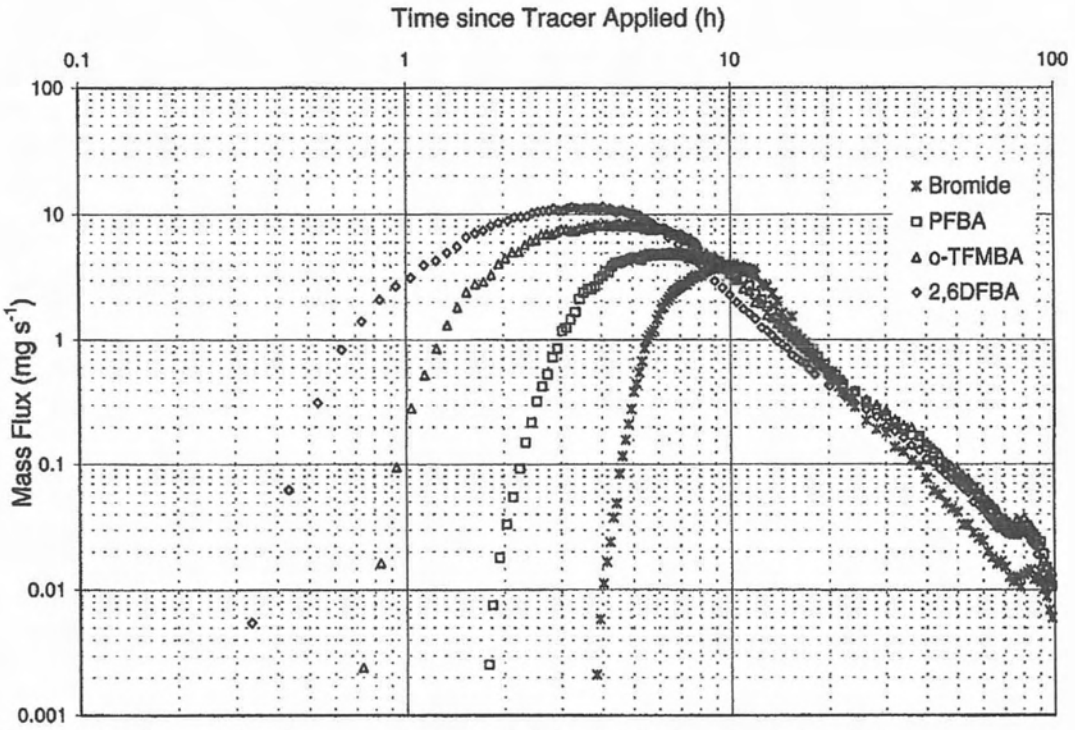

Fig. 3. The breakthrough curves of the four conservative tracers plotted against the times since their applications.

the vast leaching (i.e., 1 d) would not likely provide time for significant N transformations and uptake to occur. Our data suggested that, after the application of nitrate fertilizer in spring to a relatively dry soil surface, as much as 7% of nitrate could be leached out of a root zone by a single 10-h precipitation event as mild as 3 mm h^{-1}. On the other hand, if the nitrate were applied to relatively wet soil surface, as much as 20% could be rapidly leached out from a root zone after a mild precipitation event. This strongly suggested that highly soluble agrichemicals such as nitrate should never be applied to a wet soil surface. The question then becomes how wet is "wet"? In most cases it is impractical for N fertilizer to be applied in the middle of a rainstorm or immediately following 1.8 cm rain, as was 2,6-DFBA, but how long a delay would be required before the chemical behavior matches that of the Br^- in this experiment is unknown. The current experiment cannot answer that question. The data do clearly indicate that *fertigation* of nitrate on wet soils could lead to substantial losses of compounds through preferential flow.

The fast arrival time and the vast transport during the first day after precipitation strongly suggested that, in order to collect representative samples to assess total deep leaching, it was extremely critical to intensively monitor contaminant transport during the first day after a rainfall event. Soil sampling protocols based on the coring method of collecting soil samples at random locations once every several days is inadequate to determine contaminant leaching under field conditions. On the other hand, a field where the tiles are installed with even spacing and depth and border tiles are installed to partition the water input area would behave like a huge, enclosed and undisturbed lysimeter. Water and contaminants leached from such fields can be accurately and holistically assessed, regardless of how rapidly and preferentially the contaminants are being transported downward.

The mass flux of each tracer plotted against time since application is shown in Fig. 3 (for Br^-, time coincides with the onset of irrigation). The results show that the BTCs shifted toward the left when a tracer was applied to wetter soil during a precipitation event. Jury (1982) proposed to derive the travel-time probability density function from the tracer breakthrough patterns. The physical factors that determine the travel time under field conditions encompass the size spectrum of hydraulically active pores, chemical retardation and transformation, uptake, and degradation. Results from this study showed that much of the mass that would be leached out from a root zone was leached through preferential flow paths within the first 24 h of a precipitation. Furthermore, Kung et al. (2000) showed that the initial transport of an adsorbing tracer was almost identical to that of a non-adsorbing tracer. These results together suggested that chemical retardation, transformation, uptake, and degradation had only secondary effects in determining the initial deep leaching of agrichemicals through preferential flow paths. Under this condition, the travel-time probability density function is dictated by the field-scale size spectrum of hydraulically active pores of the preferential flow paths.

Kladivko et al. (1991) observed that a pesticide was most susceptible to deep leaching shortly after its appli-

cation. Most pesticides are applied in spring when soil water content near the soil surface varies greatly. If a pesticide were applied to a relatively dry soil surface, the Br^- breakthrough pattern would reflect the most relevant water flux distribution of preferential paths that contribute to the pesticide leaching. However, if a pesticide were applied to a wet soil surface, the water flux distribution of preferential paths reflected by the breakthrough patterns of the three benzoic acids would become more relevant in predicting the total deep leaching.

CONCLUSIONS

A preliminary study was conducted using a tile drain facility to monitor breakthrough patterns of Br^-, Cl^-, PFBA, *o*-TFMBA, and 2,6-DFBA, and nitrate applied to a silt loam soil. The similarity of all BTCs suggested that the three fluorobenzoic acids were as conservative tracers as are Br^- and Cl^- under field conditions. A tile drain facility in an adjacent plot was used to monitor breakthrough of Br^- and the three fluorobenzoic acids sequentially applied during a 10-h precipitation event with 3 mm h^{-1} intensity. The overall results showed that the impact of the water dynamics of preferential flow paths on contaminant transport can be quantified by the breakthrough patterns of sequentially applied conservative tracers. The water flux distribution of preferential flow paths was not a stationary property of a soil profile but depended primarily on soil water content of the soil profile. Each rainfall event may have a different impact on the contaminant transport through preferential paths. Specific results indicated the following:

1. The tile flow increased at around 3 h after irrigation started; Br^- breakthrough patterns started around 4 h after irrigation started. The three benzoic acids, PFBA, *o*-TFMBA, and 2,6-DFBA, were detected in the tile drainage at 102 min, 42 min, and 18 min after their applications, respectively. These patterns of fast arrival times of sequentially applied tracers proved that preferential flow dictates the deep leaching of agrichemicals.
2. The percentages of total applied mass of the tracer recovered from tile drainage were as follows: Br^- (7.04%), PFBA (13.9%), o-TFMBA, (18.7%), and 2,6-DFBA (19.7%). The fact that Br^- had the least mass leached and the 2,6-DFBA had the most was consistent with their arrival times; i.e., Br^- arrived the latest and the 2,6-DFBA arrived the earliest after their applications. This demonstrated that a contaminant moves through the preferential flow paths with larger pores when a soil profile becomes wetter during a precipitation event.
3. The fact that 90% of the deep leaching after a prolonged precipitation event occurred during the first day suggested that tracer behavior could be used to model leaching of recently applied nitrate, since there would be little time for N transformation and uptake to occur. This implied that, after the application of nitrate fertilizer in spring to a relatively dry soil surface, as much as 7% of the nitrate could be quickly leached from a root zone by a single 10-h precipitation event as mild as 3 mm h^{-1}. On the other hand, if the nitrate was applied to a relatively wet soil surface through fertigation, as much as 20% could be rapidly leached out of a root zone.
4. Because contaminant transport is dictated by fast flow through preferential paths, it was extremely critical to intensively monitor contaminant transport during the first day of a rainfall event in order to collect representative samples to assess total deep leaching. Soil sampling protocol based on the coring method of collecting soil samples at random locations once every several days is completely unsuitable to determine deep leaching of agrichemicals under field conditions. On the other hand, a tiled field behaves like a huge, enclosed, independent and undisturbed lysimeter. Contaminants leached from such a field can be accurately and holistically assessed, regardless of how rapidly and preferentially contaminants are being transported downward.

ACKNOWLEDGMENTS

Research supported by the USDA-NRICGP grant 96-35102-3773. The views and conclusions contained in this document are those of the authors and should not be interpreted as representing the official policies, either expressed or implied, of the U.S. Government. The authors gratefully acknowledge the field assistance of Mr. C. Kiefer, L. Theller, D. Szejba, D. Bauerle, D. Biehle, W. Maschino, and Drs. H. Montas and R. Hartwig, and the lab assistance of Ms. L. McKee.

REFERENCES

Alexander, R.B., R.A. Smith, and G.E. Schwarz. 1995. The regional transport of point and nonpoint-source nitrogen to the Gulf of Mexico. p.127–132. *In* Proc. of the First Gulf of Mexico Hypoxia Manage. Conf., Hypoxia in the Northern Gulf of Mexico: Past, present and future. Kenner, LA. 5–6 Dec. 1995. Available at http://www.gmpo.gov/nutrient/front.html. (verified 11 May 2000).

Bowman, R.S., and J.F. Gibbens. 1992. Difluorobenzoates as nonreactive tracers in soil and groundwater. Ground Water 30:8–14.

Casper, D.A., and K-J.S. Kung. 1996. Forward modeling to simulate the ground-penetrating radar patterns in heterogeneous sandy soils. Geophysics 64:1034–1049.

Czapar, G.F., R.S. Kanwar, and R.S. Fawcett. 1994. Herbicide and tracer movement to field drainage tiles under simulated rainfall conditions. Soil Tillage Res. 30:19–32.

Everts, C.J., R.S. Kanwar, E.C. Alexander Jr., and S.C. Alexander. 1989. Comparison of tracer mobilities under laboratory and field conditions. J. Environ. Qual. 18:491–498.

Gerke, H.H., and M.Th. van Genuchten. 1993. A dual-porosity model for simulating preferential movement of water and solutes in structured porous media. Water Resour. Res. 29:305–319.

Ghodrati, M., and W.A. Jury. 1990. A field study using dyes to characterize preferential flow of water. Soil Sci. Soc. Am. J. 54:1558–1563.

Gwo, J.P., P.M. Jardine; G.V. Wilson, and G.T. Yeh. 1995. A multiple-pore-region concept to modeling mass transfer in subsurface media. J. Hydrol. (Amsterdam) 164:217–237.

Jaynes, D.B. 1994. Evaluation of fluoro-benzoate tracers in surface soils. Ground Water 32:532–538.

Ju, S-H., and K-J.S. Kung. 1993. Finite element simulation of funnel flow and overall flow property induced by multiple soil layers. J. Environ. Qual. 22:432–442.

Ju, S-H., and K-J.S. Kung. 1997. Steady-state funnel flow: Its characteristics and impact on modeling. Soil Sci. Soc. Am. J. 61:428–435.

Ju, S-H., K-J.S. Kung, and C. Helling. 1997. Simulating impact of funnel flow on contaminant sampling in sandy soils. Soil Sci. Soc. Am. J. 61:409–415.

Jury, W.A. 1982. Simulation of solute transport using a transfer function model. Water Resour. Res. 18:363–368.

Kladivko, E.J., G.E. Van Scoyoc, E.J. Monke, K.M. Oates, and W. Pask. 1991. Pesticide and nutrient movement into subsurface tile drains on a silt loam soil in Indiana. J. Environ. Qual. 20:264–270.

Kladivko, E.J., J. Grochulska, R.F. Turco, G.E. VanScoyoc, and J.D. Eigel. 1999. Pesticide and nitrate transport into subsurface tile drains of different spacings. J. Environ. Qual. 28:997–1004.

Kung, K-J.S. 1990. Preferential flow in a sandy vadose zone: 1. Field observation & 2. Mechanism and implications. Geoderma 46:51–71.

Kung, K-J.S. 1993. Laboratory observation of the funnel flow mechanism and its influence on solute transport. J. Environ. Qual. 22: 91–102.

Kung, K-J.S., and Z-B. Lu. 1993. Using ground-penetrating radar to detect layers with abrupt discontinuity in dielectric constant from their surroundings. Soil Sci. Soc. Am. J. 57:335–340.

Kung, K-J.S., T.S. Steenhuis, E.J. Kladivko, G. Bubenzer, T. Gish, and C.S. Helling. 2000. Impact of preferential flow on the transport of adsorbing and non-adsorbing tracers. Soil Sci. Soc. Am. J. 64:1290–1296 (this issue).

Richards, T.L., and T.S. Steenhuis. 1988. Tile drain sampling of preferential flow on a field scale. *In* P.F. Germann (ed.) Rapid and far reaching hydrological processes in the vadose zone. J. Contam. Hydrol. 3:307–325.

Skopp, J., and A.W. Warrick. 1974. Two-phase model for the miscible displacement of reactive solutes in soils. Soil Sci. Soc. Am. J. 38:545–551.

USDA-NRCS. 1996. A geography of hope: America's private land. Progam aid 1548. U.S. Gov. Print. Office, Washington, DC.